

Explaining the $B_{d(s)} \rightarrow K^{(*)} \bar{K}^{(*)}$ puzzle via chiral-flip in R -parity violating MSSM with seesaw mechanism

Min-Di Zheng^{1*}, Qi-Liang Wang^{1†}, Li-Fen Lai^{1‡}, and Hong-Hao Zhang^{2§}

¹ School of Physical Science and Intelligent Education,
Shangrao Normal University, Shangrao 334001, China

² School of Physics, Sun Yat-Sen University, Guangzhou 510275, China

Abstract

We study the non-leptonic puzzle of $B_{d(s)} \rightarrow K^{(*)} \bar{K}^{(*)}$ decay in the R -parity violating minimal supersymmetric standard model (RPV-MSSM) extended with the inverse seesaw mechanism. In this model, the chiral flip of sneutrinos can contribute to the observables $L_{K\bar{K}}$ and $L_{K^*\bar{K}^*}$, that is benefit for explaining the relevant puzzle. We also find that this unique effect can engage in the B_s - \bar{B}_s mixing. We utilize the scenario of complex λ' couplings to fulfill the recent stringent constraint of B_s - \bar{B}_s mixing, and examine other related bounds of B , K -meson decays, lepton decays, neutrino data, Z decays, oblique parameters, CP violations (CPV), etc. Besides, inspired by the new measurement of $\mathcal{B}(B^+ \rightarrow K^+ \nu \bar{\nu})$ by Belle II, which shows about 2.7σ higher than the Standard Model (SM) prediction, we also investigate the New Physics (NP) enhancement to this observable.

*zhengmd5@mail.sysu.edu.cn

†wangqiliang2024@163.com

‡lailifen@mails.ccnu.edu.cn

§zhh98@mail.sysu.edu.cn

1 Introduction

In recent years, series of deviations between the experimental measurements and the SM predictions have been witnessed in the context of B -meson semileptonic decays, e.g. the lepton flavor universality (LFU) ratios $R_{D^{(*)}}$. However, another type of LFU ratios, $R_{K^{(*)}}$ within the $b \rightarrow s \ell^+ \ell^-$ ($\ell = e, \mu$) processes, has recently been reported in agreement with SM predictions [1], and it is already erased from the anomaly list. Since the LFU violation from the NP still needs time to be confirmed, there exist U-spin related observables within rare $b \rightarrow s(d)$ transitions, i.e. $L_{K^{(*)}\bar{K}^{(*)}}$ [2], which can also be utilized to search for NP clues. The observables $L_{K^{(*)}\bar{K}^{(*)}}$, defined as the ratios of longitudinal branching ratios ($\bar{B}_s^{(*)} \rightarrow K^{(*)}\bar{K}^{(*)}$ versus $\bar{B}_d^{(*)} \rightarrow K^{(*)}\bar{K}^{(*)}$), are recently measured [3–9]:

$$L_{K^*\bar{K}^*}^{\text{exp}} = 4.43 \pm 0.92, \quad L_{K\bar{K}}^{\text{exp}} = 14.58 \pm 3.37, \quad (1.1)$$

showing the $2.6\sigma(2.4\sigma)$ pull values corresponding to the SM predictions within QCD factorisation [2]:

$$L_{K^*\bar{K}^*}^{\text{SM}} = 19.53_{-6.64}^{+9.14}, \quad L_{K\bar{K}}^{\text{SM}} = 26.00_{-3.59}^{+3.88}. \quad (1.2)$$

This puzzle implies that there may exist new quark-flavor structure in NP. For the model-independent discussion, the Lagrangian of the low energy effective field theory is given by

$$\mathcal{L}_{\text{eff}} = \frac{4G_F}{\sqrt{2}} \eta_t \sum_i C_i \mathcal{O}_i + \text{h.c.}, \quad (1.3)$$

where the Cabibbo–Kobayashi–Maskawa (CKM) factor $\eta_t \equiv K_{tb}K_{tp}^*$ ($p = s, d$). The most relevant operators for the puzzle-explanation are the given QCD penguin operators and magnetic operators [10],

$$\begin{aligned} \mathcal{O}_{4p} &= (\bar{p}_L^\alpha \gamma^\mu b_L^\beta) \sum_q (\bar{q}_L^\beta \gamma_\mu q_L^\alpha), & \mathcal{O}_{6p} &= (\bar{p}_L^\alpha \gamma^\mu b_L^\beta) \sum_q (\bar{q}_R^\beta \gamma_\mu q_R^\alpha), \\ \mathcal{O}_{7\gamma p} &= \frac{-em_b}{16\pi^2} (\bar{p}_L^\alpha \sigma^{\mu\nu} b_R^\alpha) F_{\mu\nu}, & \mathcal{O}_{8gp} &= \frac{-g_s m_b}{16\pi^2} (\bar{p}_L^\alpha \sigma^{\mu\nu} T_{\alpha\beta}^a b_R^\beta) G_{\mu\nu}^a, \end{aligned} \quad (1.4)$$

where α, β are color indices and a summation over $q = u, d, c, s, b$ is implied, with the vertex couplings $+ig_s T^a$ and $+iQ_e e$ for $Q_e = -1$. The recent global fit results [2, 11, 12] show that, for

the 1σ level, ones need the negative C_{8gs}^{NP} (positive C_{8gd}^{NP}) with the value of $\mathcal{O}(10^{-1})$, or positive C_{4s}^{NP} (negative C_{4d}^{NP}) with the value of $\mathcal{O}(10^{-2})$, while single positive C_{6s}^{NP} around $\mathcal{O}(10^{-2})$ can only explain the tension of $L_{K\bar{K}}$.

Since the recent model-independent researches throw light on the regions of Wilson coefficients, in this work, we will investigate this puzzle in a concrete NP model. Inspired by the recent research on the gluon-penguin contributions, within the S_1 -leptoquark model containing the $U(q)_{1,2}$ flavor symmetry and inverse seesaw mechanism [13], we utilize the RPV-MSSM extended with the inverse seesaw mechanism (named as RPV-MSSMIS). It is worth mentioning that we had recently proposed this model to study LFU observables, i.e. $R_{K^{(*)}}$ and $R_{D^{(*)}}$, as well as the muon anomalous magnetic moment [14, 15], and this model can provide the particular feature for different quark flavor through the λ' -coupling texture. In this work, we find that the chiral flip of sneutrino can make unique contributions to the Wilson coefficients $C_{8gs(d)}^{\text{NP}}$, extracted from the gluon-penguin diagrams, through mainly the $\tilde{\nu}dd$ loop. Also, the strict constraint from the rare decay $B \rightarrow X_s\gamma$, can be relaxed by the cancellation of $C_{8gs(d)}^{\text{NP}} = -3C_{7\gamma s(d)}^{\text{NP}}$ (this relation is induced by the model feature). In this work, we scrutinize all the one-loop gluon(γ)-penguin diagrams of b interaction to $s(d)$, as well as the calculations in other related processes, within the RPV-MSSMIS. Among these, we also find significant chiral-flip contribution to the $B_s\text{--}\bar{B}_s$ mixing, and this effect on $B \rightarrow K^{(*)}\nu\bar{\nu}$ decays. Recently, Belle II Collaboration has reported the new measurement of the branching ratio, $\mathcal{B}(B^+ \rightarrow K^+\nu\bar{\nu})_{\text{exp}} = (2.3 \pm 0.7) \times 10^{-5}$ [16], higher than the corresponding SM prediction [17] by around 2.7σ . As is known to all, this b decaying into s mode is one of the cleanest probes for NP searches due to its highly suppressed theoretical uncertainty. Here we revisit the NP contributions to the $b \rightarrow s\nu\bar{\nu}$ transition and discuss the enhancement effects.

This paper is organized as follows. The RPV-MSSMIS model and the theoretical calculations are in Sec. 2. Then, in Sec. 3, we scrutinize the related constraints, which are followed by numerical results and discussions in Sec. 4 and additional discussions on CPV in Sec. 5. Our conclusions are presented in Sec. 6.

2 The tension study in RPV-MSSMIS

In this section, the NP effects, especially the chiral-flip ones, are investigated in the $B_{d(s)} \rightarrow K^{(*)}\bar{K}^{(*)}$ and $B \rightarrow K^{(*)}\nu\bar{\nu}$ decays, within the RPV-MSSMIS.

2.1 RPV-MSSMIS framework

First let us briefly review the RPV-MSSMIS [14]. Here are given the superpotential and the soft supersymmetric (SUSY) breaking Lagrangian,

$$\begin{aligned}\mathcal{W} = & \mathcal{W}_{\text{MSSM}} + Y_\nu^{ij} \hat{R}_i \hat{L}_j \hat{H}_u + M_R^{ij} \hat{R}_i \hat{S}_j + \frac{1}{2} \mu_S^{ij} \hat{S}_i \hat{S}_j + \lambda'_{ijk} \hat{L}_i \hat{Q}_j \hat{D}_k, \\ \mathcal{L}^{\text{soft}} = & \mathcal{L}_{\text{MSSM}}^{\text{soft}} - (m_{\tilde{R}}^2)_{ij} \tilde{R}_i^* \tilde{R}_j - (m_{\tilde{S}}^2)_{ij} \tilde{S}_i^* \tilde{S}_j \\ & - (A_\nu Y_\nu)_{ij} \tilde{R}_i^* \tilde{L}_j H_u - B_{MR}^{ij} \tilde{R}_i^* \tilde{S}_j - \frac{1}{2} B_{\mu_S}^{ij} \tilde{S}_i \tilde{S}_j,\end{aligned}\quad (2.1)$$

where the generation indices $i, j, k = 1, 2, 3$ while the colour ones are omitted, and squarks (sleptons) are denoted by the symbol “ \sim ”, and as for the MSSM parts, $\mathcal{W}_{\text{MSSM}}$ and $\mathcal{L}_{\text{MSSM}}^{\text{soft}}$, the reader can refer to Refs [18, 19]. All repeated indices are assumed to be summed over throughout this paper unless otherwise stated. The neutral scalar fields of the two Higgs doublet superfields, $\hat{H}_u = (\hat{H}_u^+, \hat{H}_u^0)^T$ and $\hat{H}_d = (\hat{H}_d^0, \hat{H}_d^-)^T$, acquire the non-zero vacuum expectation value, i.e. $\langle H_u^0 \rangle = v_u$ and $\langle H_d^0 \rangle = v_d$, respectively, and their mixing is expressed by $\tan \beta = v_u/v_d$.

The neutrino sector in the superpotential \mathcal{W} provides the neutrino mass spectrum at the tree level, and in the (ν, R, S) basis, the 9×9 mass matrix \mathcal{M}_ν is given by

$$\mathcal{M}_\nu = \begin{pmatrix} 0 & m_D^T & 0 \\ m_D & 0 & M_R \\ 0 & M_R^T & \mu_S \end{pmatrix}, \quad (2.2)$$

where the Dirac mass matrix $m_D = \frac{1}{\sqrt{2}} v_u Y_\nu^T$. Then ones can diagonalize \mathcal{M}_ν through $\mathcal{M}_\nu^{\text{diag}} = \mathcal{V} \mathcal{M}_\nu \mathcal{V}^T$. As to the sneutrino mass square matrix $\mathcal{M}_{\tilde{\nu}^{\mathcal{I}(\mathcal{R})}}^2$ in the $(\tilde{\nu}_L^{\mathcal{I}(\mathcal{R})}, \tilde{R}^{\mathcal{I}(\mathcal{R})}, \tilde{S}^{\mathcal{I}(\mathcal{R})})$ basis, it is expressed as

$$\begin{aligned}\mathcal{M}_{\tilde{\nu}^{\mathcal{I}(\mathcal{R})}}^2 = & \begin{pmatrix} m_{\tilde{L}'}^2 & (A_\nu - \mu \cot \beta) m_D^T & m_D^T M_R \\ (A_\nu - \mu \cot \beta) m_D & m_{\tilde{R}}^2 + M_R M_R^T + m_D m_D^T & \pm M_R \mu_S + B_{MR} \\ M_R^T m_D & \pm \mu_S M_R^T + B_{MR}^T & m_{\tilde{S}}^2 + \mu_S^2 + M_R^T M_R \pm B_{\mu_S} \end{pmatrix} \\ \approx & \begin{pmatrix} m_{\tilde{L}'}^2 & (A_\nu - \mu \cot \beta) m_D^T & m_D^T M_R \\ (A_\nu - \mu \cot \beta) m_D & m_{\tilde{R}}^2 + M_R M_R^T + m_D m_D^T & B_{MR} \\ M_R^T m_D & B_{MR}^T & m_{\tilde{S}}^2 + M_R^T M_R \pm B_{\mu_S} \end{pmatrix},\end{aligned}\quad (2.3)$$

where the “ \pm ”, as well as “ $\mathcal{R}(\mathcal{I})$ ”, denotes the even (odd) CP, and the mass square $m_{\tilde{L}'}^2 \equiv$

$m_L^2 + \frac{1}{4}g_2^2 v^2 \cos 2\beta + m_D m_D^T$ is regarded as the model input, with m_L^2 being the soft mass square of \tilde{L} . The parameter μ_S is generally tiny inducing the smallness of active neutrino mass [20], while B_{μ_S} is considered non-negligible, which induces the mass splitting between the CP-even and CP-odd sneutrinos for the same flavor. This is different from the degenerate-mass approximation adopted in our recent researches [14, 15]¹. In the following sections, ones will see that this splitting-mass scenario can provide the chiral-flip contributions in some processes.

Afterwards we introduce the trilinear RPV interaction in this model. The superpotential term $\lambda'_{ijk} \hat{L}_i \hat{Q}_j \hat{D}_k$ induces the relevant Lagrangian in the context of mass eigenstates for the down-type quarks and charged leptons, which is given by

$$\begin{aligned} \mathcal{L}_{\text{LQD}} = & \lambda_{vjk}^{\mathcal{I}(\mathcal{R})} \tilde{\nu}_v^{\mathcal{I}(\mathcal{R})} \bar{d}_{Rk} d_{Lj} + \lambda_{vjk}^{\mathcal{N}} (\tilde{d}_{Lj} \bar{d}_{Rk} \nu_v + \tilde{d}_{Rk}^* \bar{\nu}_v^c d_{Lj}) \\ & - \tilde{\lambda}'_{ilk} (\tilde{l}_{Li} \bar{d}_{Rk} u_{Ll} + \tilde{u}_{Ll} \bar{d}_{Rk} l_{Li} + \tilde{d}_{Rk}^* \bar{l}_{Li}^c u_{Ll}) + \text{h.c.}, \end{aligned} \quad (2.4)$$

where “ c ” indicates the charge conjugated fermions, and the fields $\tilde{\nu}_L^{\mathcal{I}(\mathcal{R})}$, ν_L , and u_L (aligned with \tilde{u}_L) in the flavor basis have been rotated into mass eigenstates by the mixing matrices $\tilde{\mathcal{V}}^{\mathcal{I}(\mathcal{R})}$, \mathcal{V} , and K , respectively. Besides, the index $v = 1, 2, \dots, 9$ denotes the generation of the physical (s)neutrinos, and the three λ' couplings are deduced as $\lambda_{vjk}^{\mathcal{I}(\mathcal{R})} \equiv \lambda'_{ijk} \tilde{\mathcal{V}}_{vi}^{\mathcal{I}(\mathcal{R})*}$, $\lambda_{vjk}^{\mathcal{N}} \equiv \lambda'_{ijk} \mathcal{V}_{vi}$, and $\tilde{\lambda}'_{ilk} \equiv \lambda'_{ijk} K_{lj}^*$. In the following, we adopt the “single-value- k ” assumption, i.e. both λ'_{ij1} and λ'_{ij2} are set negligible, and the NP Wilson coefficients are given at the scale $\mu_{\text{NP}} = 1 \text{ TeV}$.

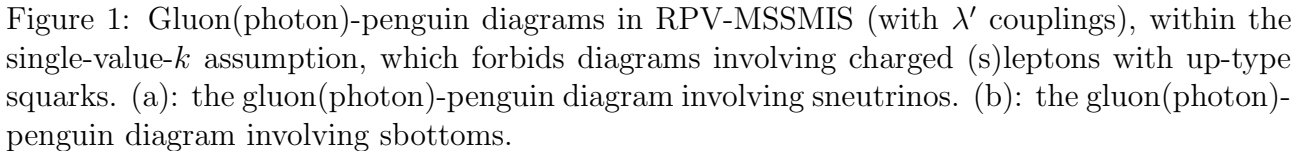
2.2 $B_{d(s)} \rightarrow K^{(*)} \bar{K}^{(*)}$ puzzle

In RPV-MSSMIS, one of the most favored operators to explain the $B_{d(s)} \rightarrow K^{(*)} \bar{K}^{(*)}$ puzzle is the magnetic one, i.e. \mathcal{O}_{8gs} , extracted from the gluon-penguins at one-loop level, shown in Fig. 1. Given that the stringent constraints from $B_s - \bar{B}_s$ mixing and $B \rightarrow X_s \gamma$ decay, which will be discussed in Sec. 3, are very sensitive to left-handed (LH) squark sector [22, 23], we set all LH-squarks with soft breaking masses above 10 TeV. So the effective contributions involve the following sparticles, i.e. sneutrinos, right-handed (RH) squarks, and gluinos, where gluinos only engage the R -parity conserved interaction. With the aid of the packages **FeynArts** [24] and **FeynCalc** [25], all the amplitudes of these gluon(photon)-penguin diagrams can be calculated. We write the model file of RPV-MSSMIS for package **SARAH** [26] to generate the model file for

¹Although the quasi-degenerate-mass scenario is favored by the direct dark matter (DM) detection [21], we focus on the field of B -meson processes, and given RPV is involved, DM is out of the scope of this work.

Next, we will show that, the NP Wilson coefficients $C_{7\gamma p}^{\text{NP}}$ and C_{8gp}^{NP} in RPV-MSSMIS can include the chiral-flip contributions, in the mass-splitting scenario mentioned in Sec. 2.1. The coefficient C_{8gp}^{NP} , extracted from the diagrams containing sneutrinos (other suppressed contributions omitted here, but all considered in the numerical calculations in Sec. 4) is given by,

and $C_{7\gamma p}^{\text{NP}}$ is calculated as $-C_{8gp}/3$ because that in the setup of this model, the difference of the NP parts between $bp\gamma$ diagram and bpg one is merely $-1/3$. In Eq. (2.5), one can find that the chiral-flip is contained in the first two terms containing double- λ'^* couplings. If we utilize the degenerate-mass scenario, these two terms totally cancel with each other, remaining the non-flip terms, $\lambda_{v23}^{\mathcal{I}*}\lambda_{v33}^{\mathcal{I}}/m_{\tilde{\nu}_v^{\mathcal{I}}}^2 + \lambda_{v23}^{\mathcal{R}*}\lambda_{v33}^{\mathcal{R}}/m_{\tilde{\nu}_v^{\mathcal{R}}}^2 = 2\lambda_{v23}^{\mathcal{I}*}\lambda_{v33}^{\mathcal{I}}/m_{\tilde{\nu}_v^{\mathcal{I}}}^2$, which agrees with the result in Ref. [27], with the formula-sign checked. Instead, if there exists a sufficient split between the masses $m_{\tilde{\nu}_v^{\mathcal{I}}}$ and $m_{\tilde{\nu}_v^{\mathcal{R}}}$ for the same v , the unique chiral-flip part is dominating, enhanced by logarithm terms. Here we analyse Fig. 1a qualitatively in the flavor basis to illustrate how double- λ'^* terms are related to the chiral-flip. First the leading order term only contains normal $\lambda'\lambda'^*$ couplings. When we consider the next order with the mixing of chirality for one single virtual quark, the chirality of sneutrino should also be flipped, inducing that double- λ'^* couplings emerge. This situation is unique since (s)neutrino chiral-flip is forbidden in original RPV-MSSM, which only contains Dirac neutrinos while no Majorana ones.



Then it is worth mentioning that we also calculate the Wilson coefficient C_{9U}^{NP} related to the operator, $\mathcal{O}_9 = \frac{e^2}{16\pi^2}(\bar{s}_L\gamma^\mu b_L)(\bar{\ell}\gamma_\mu\ell)$, which providing the lepton flavor universal contributions to $b \rightarrow s\ell^+\ell^-$, also dominated by the $\tilde{\nu}dd$ loop. The result is given that,

$$C_{9U}^{\text{NP}} = -\frac{\sqrt{2}}{144G_F\eta_t} \left\{ \frac{\lambda_{v23}^{\prime\mathcal{I}*}\lambda_{v33}^{\prime\mathcal{I}}}{m_{\tilde{\nu}_v^{\mathcal{I}}}^2} \left[\frac{8}{3} + 2\log\left(\frac{m_b^2}{m_{\tilde{\nu}_v^{\mathcal{I}}}^2}\right) \right] + \frac{\lambda_{v23}^{\prime\mathcal{R}*}\lambda_{v33}^{\prime\mathcal{R}}}{m_{\tilde{\nu}_v^{\mathcal{R}}}^2} \left[\frac{8}{3} + 2\log\left(\frac{m_b^2}{m_{\tilde{\nu}_v^{\mathcal{R}}}^2}\right) \right] + \frac{\lambda_{v23}^{\prime\mathcal{I}*}\lambda_{v33}^{\prime\mathcal{I}*}}{m_{\tilde{\nu}_v^{\mathcal{I}}}^2} - \frac{\lambda_{v23}^{\prime\mathcal{R}*}\lambda_{v33}^{\prime\mathcal{R}*}}{m_{\tilde{\nu}_v^{\mathcal{R}}}^2} \right\}, \quad (2.6)$$

and ones can find that, the chiral-flip part in Eq. (2.6), expressed by the double- λ'^* terms, is not enhanced by logarithm terms. In the degenerate-mass scenario, the result returns to the one shown in Ref. [14]. We also examine the Z -penguin contribution to C_{9U}^{NP} , and find that it is negligible in the setup of this work.

As mentioned in Sec. 1, there are divergences between the experiment data and SM results, corresponding to the non-leptonic ratios $L_{K^{(*)}\bar{K}^{(*)}}$. If we consider NP is only within $B_s \rightarrow K^{(*)}\bar{K}^{(*)}$ decays without the B_d decays, the predictions of the ratios, $L_{K^{(*)}\bar{K}^{(*)}}$, can be given by [2, 13],

$$L_{K\bar{K}}/L_{K\bar{K}}^{\text{SM}} \approx 1 + 1.13C_{8gs}^{\text{NP}}(\mu_{\text{EW}}) + 0.34C_{8gs}^{\text{NP}}(\mu_{\text{EW}})^2, \quad (2.7)$$

$$L_{K^*\bar{K}^*}/L_{K^*\bar{K}^*}^{\text{SM}} \approx 1 + 2.41C_{8gs}^{\text{NP}}(\mu_{\text{EW}}) + 1.74C_{8gs}^{\text{NP}}(\mu_{\text{EW}})^2, \quad (2.8)$$

where the electroweak (EW) broken scale $\mu_{\text{EW}} = 160$ GeV. Then at 2σ level, we need $C_{8gs}^{\text{NP}} \lesssim -0.08$ to explain the non-leptonic tension. The NP in bd sector is constrained very strictly which will be shown in Sec. 3.3.

2.3 $B \rightarrow K^{(*)}\nu\bar{\nu}$ revisited

In this section, we revisit the $B \rightarrow K^{(*)}\nu\bar{\nu}$ processes related to the quark transition $d_j \rightarrow d_m\nu_i\bar{\nu}_{i'}$, and the corresponding effective Lagrangian is,

$$\begin{aligned} \mathcal{L}_{\text{eff}}^{dd\nu\bar{\nu}} = & (C_{mj}^{\text{SM}}\delta_{ii'} + C_{mj}^{\text{NP}})(\bar{d}_m\gamma_\mu P_L d_j)(\bar{\nu}_i\gamma^\mu P_L \nu_{i'}) + C_{mj}^{\text{1SRR}}(\bar{d}_m P_R d_j)(\bar{\nu}_i P_R \nu_{i'}) \\ & + C_{mj}^{\text{2SRR}}(\bar{d}_m\sigma_{\mu\nu} P_R d_j)(\bar{\nu}_i\sigma^{\mu\nu} P_R \nu_{i'}) + \text{h.c.}, \end{aligned} \quad (2.9)$$

where the SM contribution is $C_{mj}^{\text{SM}} = -\frac{\sqrt{2}G_F e^2 K_{tj} K_{tm}^*}{4\pi^2 \sin^2 \theta_W} X(x_t)$ and the loop function $X(x_t) \equiv \frac{x_t(x_t+2)}{8(x_t-1)} + \frac{3x_t(x_t-2)}{8(x_t-1)^2} \log(x_t)$ with $x_t \equiv m_t^2/m_W^2$ [28]. The NP contribution of vector current is [15]

$$C_{mj}^{\text{NP}} = \frac{\lambda_{i'j3}^{\mathcal{N}} \lambda_{im3}^{\mathcal{N}*}}{2m_{\tilde{b}_R}^2} = \frac{\mathcal{V}_{i'\alpha'} \mathcal{V}_{i\alpha}^* \lambda_{\alpha'j3}^{\mathcal{N}} \lambda_{\alpha m3}^{\mathcal{N}*}}{2m_{\tilde{b}_R}^2}. \quad (2.10)$$

Besides, the NP coefficients $C_{mj}^{1\text{SRR}}$ and $C_{mj}^{2\text{SRR}}$ express the chiral-flip contributions of neutrino with sbottoms. However, the global fit shows that, these scalar and tensor contributions are negligible, relative to the vector one [29]. For simplicity, we consider negligible mixing for the \tilde{b} sector to omit these two coefficients.

To study the NP effects on $B^+ \rightarrow K^+ \nu \bar{\nu}$ as well as $B \rightarrow K^* \nu \bar{\nu}$, ones can define the ratio, $R_{K^{(*)}}^{\nu \bar{\nu}} \equiv \mathcal{B}(B \rightarrow K^{(*)} \nu \bar{\nu}) / \mathcal{B}(B \rightarrow K^{(*)} \nu \bar{\nu})_{\text{SM}}$. In RPV-MSSMIS, we get that,

$$R_K^{\nu \bar{\nu}} = R_{K^*}^{\nu \bar{\nu}} = \frac{\sum_{i=1}^3 |C_{23}^{\text{SM}} + C_{23}^{\text{NP}}|^2 + \sum_{i \neq i'}^3 |C_{23}^{\text{NP}}|^2}{3 |C_{23}^{\text{SM}}|^2}. \quad (2.11)$$

The recent Belle-II data [16] of $B \rightarrow K^+ \nu \bar{\nu}$, and the updated SM prediction [17], induce $R_K^{\nu \bar{\nu}} = 5.3 \pm 1.7$ [30]. Recent research [30] shows that, the case of $R_K^{\nu \bar{\nu}} = R_{K^*}^{\nu \bar{\nu}}$ cannot simultaneously fulfill the Belle-II data at 1σ level as well as the upper limit $\mathcal{B}(B \rightarrow K^* \nu \bar{\nu})_{\text{exp}} < 1.8 \times 10^{-5}$ [31], i.e. $R_{K^*}^{\nu \bar{\nu}} < 1.9$, at 90% confidence level (CL). Besides, with the theoretical result $\mathcal{B}(B^+ \rightarrow K^+ \nu \bar{\nu}) / \mathcal{B}(B \rightarrow K^* \nu \bar{\nu}) \approx 0.4$ for the single left-handed vector operator, it is also found that this case cannot explain the Belle-II data, without staying below the upper limit of $\mathcal{B}(B \rightarrow K^* \nu \bar{\nu})$ at 90% CL [32, 33]. Although 2σ -level considerations for both processes may provide room for NP in this single-operator case, in this work, we still investigate the degree of $R_K^{\nu \bar{\nu}}$ approaching to the upper limit 1.9, in the parameter space of RPV-MSSMIS.

3 The constraints

Before the numerical analysis of $B_{d(s)} \rightarrow K^{(*)} \bar{K}^{(*)}$ puzzle, the relevant theoretical and experimental constraints should also be scrutinised.

3.1 Theoretical constraints

Firstly, some theoretical constraints on the model parameters of RPV-MSSMIS should be mentioned. As one knows, the λ' couplings can be complex, although it may cause extra CP violations to some extent. With the consideration of perturbativity, $|\lambda'| \leq \sqrt{4\pi}$ should be fulfilled [34]. Moreover, the off-diagonal elements of the scalar-field trilinear couplings in the soft-breaking terms, e.g. A_u in the soft-breaking term $A_u H_u \tilde{Q} \tilde{U}$, are severely restricted by the dangerous charge and colour breaking (CCB) minima and unbounded from below directions (UFB) in the effective potential [35–38]. Thus, all the flavour-violating off-diagonal elements in the chiral-mixing sectors are set negligible, because the CCB and UFB bounds on them are always stronger than the ones from flavour-changing neutral-current processes, and even do not decrease when the SUSY scale increases [35–37]. As for the seesaw part of this model, we consider the perturbative unitarity [39–43], which constrains the heavy-neutrino parameter space, i.e. the mixing matrix \mathcal{V} and heavy neutrino masses. This bound restricts the heavy neutrino decay width to comply with $\Gamma(N_v)/m_{N_v} < \frac{1}{2}$, ($v \geq 4$). For $\mathcal{V}_{vi} \sim \mathcal{O}(10^{-2})$, the main contribution to $\Gamma(N_v)$ is the $N \rightarrow Wl$ decay ($v \geq 4$), and at tree level, it is given by [44],

$$\Gamma(N_v \rightarrow Wl_i) = \frac{e^2}{64\pi \sin^2 \theta_W} |\mathcal{V}_{vi}|^2 \frac{\lambda^{1/2}(m_{N_v}^2, M_W^2, m_{l_i}^2)}{m_{N_v}} \left[1 + \frac{m_{l_i}^2 - 2M_W^2}{m_{N_v}^2} + \frac{(m_{N_v}^2 - m_{l_i}^2)^2}{m_{N_v}^2 M_W^2} \right], \quad (3.1)$$

where the Källén function $\lambda(a, b, c) = [a - (\sqrt{b} - \sqrt{c})^2][a - (\sqrt{b} + \sqrt{c})^2]$. The decay widths of $N_v \rightarrow ZN_{v'}$ and $N_i \rightarrow HN_j$ (H is SM Higgs) are both proportional to the coupling $\Sigma_i \mathcal{V}_{vi}^* \mathcal{V}_{vi}$ [44], and they are suppressed strongly.

3.2 Direct searches

Then, we move on to the experimental constraints and direct searches for SUSY particles should be considered first. Since there are no signs of NP particles until the end of the LHC run II, which reaches around 140 fb^{-1} at the center energy 13 TeV, providing stringent bounds on SUSY models. The allowed masses of colored sparticles, such as gluinos, the first-two generation squarks, stops and sbottoms have been excluded up to $1 - 2 \text{ TeV}$ scale [45–51]. In this work, the masses of LH-squarks are set above 10 TeV, whereas the masses of sleptons as well as the heavy neutrinos are all around $10^2 - 10^3 \text{ GeV}$. Some recent experiments have pushed the upper limit of slepton masses over TeV scale [52–54], however, these searches consider nonzero λ related

to the superpotential $\lambda_{ijk}\hat{L}_i\hat{L}_j\hat{E}_k$. Given that we only consider nonzero λ' in the model, this bound can be relaxed. It is worth mentioning that, ATLAS has recently made searches for the NP signs of this type of model, only containing λ' couplings [55]. Using the first collider limits for this model type, we keep $m_{\tilde{\mu}} \gtrsim 470$ GeV.

3.3 Tree-level processes

Next, we check the tree-level processes exchanging sbottoms, including $K^+ \rightarrow \pi^+\nu\bar{\nu}$, $B \rightarrow \pi\nu\bar{\nu}$, $D^0 \rightarrow \ell^+\ell^-$, $\tau \rightarrow \ell\rho^0$ as well as $B \rightarrow \tau\nu$, $D_s \rightarrow \tau\nu$, $\tau \rightarrow K(\pi)\nu$ and $\pi \rightarrow \ell\nu(\gamma)$.

As one knows that the experimental measurement $\mathcal{B}(K^+ \rightarrow \pi^+\nu\bar{\nu})_{\text{exp}} = (1.14_{-0.33}^{+0.40}) \times 10^{-10}$ [56] and the SM prediction $\mathcal{B}(K^+ \rightarrow \pi^+\nu\bar{\nu})_{\text{SM}} = (9.24 \pm 0.83) \times 10^{-11}$ [57] induce the strong constraint, $|\lambda'_{i'2k}\lambda'_{i1k}| \lesssim 10^{-4}(m_{\tilde{b}_R}/1\text{TeV})^2$. Even for \tilde{b}_R with 10 TeV mass, there still exists the bound of $|\lambda'_{i'2k}\lambda'_{i1k}| \lesssim 0.01$. Thus, we assume λ'_{i1k} negligible to avoid this bound from this process, as well as the $B \rightarrow \pi\nu\bar{\nu}$ decay.

In table 1, we collect the experimental results and SM predictions of $D^0 \rightarrow \ell^+\ell^-$, $\tau \rightarrow \ell\rho^0$ decays with the charged current processes, $B \rightarrow \tau\nu$, $D_s \rightarrow \tau\nu$ and $\tau \rightarrow K\nu$, as well as the processes discussed above. Following the same/analogical numerical calculations in the ordinary RPV-MSSM (see Refs. [58, 59]), we update the constraint from $\mathcal{B}(D^0 \rightarrow \mu^+\mu^-)$, as $|\lambda'_{223}|^2 < 0.22(m_{\tilde{b}_R}/1\text{TeV})^2$, and the bound from $\mathcal{B}(D^0 \rightarrow e^+e^-)$ is negligible due to the small m_e . We also update the calculation of the process $\mathcal{B}(\tau \rightarrow \ell\rho^0)$, which provides the bound $|\lambda'_{323}\lambda'_{223}| < 0.45(m_{\tilde{b}_R}/1\text{TeV})^2$ as well as $|\lambda'_{323}\lambda'_{123}| < 0.51(m_{\tilde{b}_R}/1\text{TeV})^2$. The functions R_{133} , R_{223} , and R_{123} (see concrete definitions in Ref. [59]), are utilized to express the ratios of the measurement values versus the SM predictions for $\mathcal{B}(B \rightarrow \tau\nu)$, $\mathcal{B}(D_s \rightarrow \tau\nu)$, and $\mathcal{B}(\tau \rightarrow K\nu)$, respectively, and we also consider these constraints.

As for the $\pi \rightarrow \ell\nu(\gamma)$ decay, similar to the formula in Ref. [60], the bound (here also including λ' -loop corrections) can be shown with

$$\frac{1 + \eta_{\mu\mu} + h'_{\mu\mu}}{1 + \eta_{ee} + h'_{ee}} = 1.0010(9), \quad (3.2)$$

where the function η and h' express the non-unitary part of neutrino and λ' -loop corrections to $Wl\nu$ -vertex, respectively, and they are given by [15]

$$\eta_{ij} \equiv (\mathcal{V}_{3 \times 3}^T)_{ik} \mathcal{U}_{kj}^{-1} - \delta_{ij},$$

Observations	SM predictions	Experimental data
$\mathcal{B}(K^+ \rightarrow \pi^+ \nu \bar{\nu})$	$(9.24 \pm 0.83) \times 10^{-11}$ [57]	$(1.14^{+0.40}_{-0.33}) \times 10^{-10}$ [56]
$\mathcal{B}(D^0 \rightarrow \mu^+ \mu^-)$	$\lesssim 6 \times 10^{-11}$ [63]	$< 3.1 \times 10^{-9}$ [64]
$\mathcal{B}(\tau \rightarrow e \rho^0)$	-	$< 2.2 \times 10^{-8}$ [65]
$\mathcal{B}(\tau \rightarrow \mu \rho^0)$	-	$< 1.7 \times 10^{-8}$ [65]
$\mathcal{B}(B \rightarrow \tau \nu)$	$(9.47 \pm 1.82) \times 10^{-5}$ [66]	$(1.09 \pm 0.24) \times 10^{-4}$ [56]
$\mathcal{B}(D_s \rightarrow \tau \nu)$	$(5.40 \pm 0.30)\%$ [59]	$(5.36 \pm 0.10)\%$ [56]
$\mathcal{B}(\tau \rightarrow K \nu)$	$(7.15 \pm 0.026) \times 10^{-3}$ [67]	$(6.96 \pm 0.10) \times 10^{-3}$ [56]

Table 1: Current status of the relevant processes which can be affected by RPV-MSSMIS at tree level. The experimental upper limits are given at 90% CL.

$$h'_{li} = -\frac{3}{64\pi^2} x_{\tilde{b}_R} f_W(x_{\tilde{b}_R}) \tilde{\lambda}'_{i33} \tilde{\lambda}'_{i33}, \quad (3.3)$$

where \mathcal{U} is unitary Pontecorvo–Maki–Nakagawa–Sakata (PMNS)-like, and the loop function $f_W(x) \equiv \frac{1}{x-1} + \frac{(x-2)\log x}{(x-1)^2}$ with $x_{\tilde{b}_R} \equiv m_t^2/m_{\tilde{b}_R}^2$, from the dominant $u_i d_i \tilde{b}_R$ -loop diagram. In the inverse seesaw framework, the Hermitian η can be figured out, i.e. $\eta \approx -\frac{1}{2} m_D^\dagger (M_R^*)^{-1} (M_R^T)^{-1} m_D$. We can translate the bound Eq. (3.2) into $|\eta_{ee} + h'_{ee}| \lesssim 0.0028$ at the 2σ level, with the negligible $\eta(h')_{\mu\mu}$. In this work, we can set sufficiently small λ'_{2jk} to keep $h'_{\mu\mu}$ (negative as well as $\eta_{\mu\mu}$) negligible to avoid enlarging the Cabbibo anomaly [61, 62].

In RPV-MSSMIS, the neutrino mixing matrix, \mathcal{V} , is also bounded by the $\tau(\mu)$ decaying to charged leptons and neutrinos at the tree level. However, at one-loop level, both \mathcal{V} and λ' couplings are constrained by these decays as well as the charged lepton flavor violating (cLFV) decays. We will address $\tau(\mu)$ decays totally in the following subsection 3.4, and before that, we can make a summary that couplings λ'_{i13} and λ'_{2j3} are already set negligible (at μ_{NP} scale), considering the constraints investigated above, and that is, NP is mainly not contained in the d and μ sectors.

3.4 Loop-level processes

In this section illustrating loop-level bounds, we firstly investigate the $B_s - \bar{B}_s$ mixing, which is mastered by

$$\mathcal{L}_{\text{eff}}^{b\bar{s}b\bar{s}} = (C_{\text{SM}}^{\text{VLL}} + C_{\text{NP}}^{\text{VLL}})(\bar{s}\gamma_\mu P_L b)(\bar{s}\gamma^\mu P_L b) + C_{\text{NP}}^{1\text{SRR}}(\bar{s}P_R b)(\bar{s}P_R b) + \text{h.c.}, \quad (3.4)$$

where the SM contribution is $C_{B_s}^{\text{SM}} = -\frac{1}{4\pi^2} G_F^2 m_W^2 \eta_t^2 S(x_t)$ with the defined function $S(x_t) \equiv \frac{x_t(4-11x_t+x_t^2)}{4(x_t-1)^2} + \frac{3x_t^3 \log(x_t)}{2(x_t-1)^3}$ [59]. With the aid of **FeynArts** and **FeynCalc** packages, the non-negligible NP contributions are given by,

$$\begin{aligned} C_{\text{NP}}^{\text{VLL}} &= \frac{1}{8i} \left(\frac{1}{4} \Lambda_{vv'}^{1\mathcal{X}\mathcal{Y}} D_2[m_{\tilde{\nu}_v^{\mathcal{X}}}, m_{\tilde{\nu}_{v'}^{\mathcal{Y}}}, m_b, m_b] + \Lambda_{vv'}^{\mathcal{N}} D_2[m_{\nu_v}, m_{\nu_{v'}}, m_{\tilde{b}_R}, m_{\tilde{b}_R}] \right), \\ C_{\text{NP}}^{\text{1SRR}} &= \frac{1}{8i} \left(\Lambda_{vv'}^{2\mathcal{X}\mathcal{Y}} (-1)^{\delta_{\mathcal{X}\mathcal{Y}}+1} m_b^2 D_0[m_{\tilde{\nu}_v^{\mathcal{X}}}, m_{\tilde{\nu}_{v'}^{\mathcal{Y}}}, m_b, m_b] \right. \\ &\quad + \Lambda_{vv'}^{3\mathcal{X}\mathcal{Y}} (\delta_{\mathcal{X}\mathcal{R}} - \delta_{\mathcal{X}\mathcal{I}}) m_b^2 D_0[m_{\tilde{\nu}_v^{\mathcal{X}}}, m_{\tilde{\nu}_{v'}^{\mathcal{Y}}}, m_b, m_b] - \Lambda_{vv'}^{1\mathcal{X}\mathcal{Y}} m_b^2 D_1[m_{\tilde{\nu}_v^{\mathcal{X}}}, m_{\tilde{\nu}_{v'}^{\mathcal{Y}}}, m_b, m_b] \\ &\quad \left. + \Lambda_{vv'}^{4\mathcal{X}\mathcal{Y}} (\delta_{\mathcal{Y}\mathcal{I}} - \delta_{\mathcal{Y}\mathcal{R}}) m_b^2 D_1[m_{\tilde{\nu}_v^{\mathcal{X}}}, m_{\tilde{\nu}_{v'}^{\mathcal{Y}}}, m_b, m_b] - \frac{\lambda_{v23}^{\mathcal{I}*2}}{2m_{\tilde{\nu}_v^{\mathcal{I}}}^2} + \frac{\lambda_{v23}^{\mathcal{R}*2}}{2m_{\tilde{\nu}_v^{\mathcal{R}}}^2} \right), \end{aligned} \quad (3.5)$$

where $\Lambda_{vv'}^{1\mathcal{X}\mathcal{Y}} \equiv \lambda_{v33}^{\mathcal{X}} \lambda_{v23}^{\mathcal{X}*} \lambda_{v'33}^{\mathcal{Y}} \lambda_{v'23}^{\mathcal{Y}*}$, $\Lambda_{vv'}^{2\mathcal{X}\mathcal{Y}} \equiv \lambda_{v33}^{\mathcal{X}*} \lambda_{v23}^{\mathcal{X}} \lambda_{v'33}^{\mathcal{Y}*} \lambda_{v'23}^{\mathcal{Y}}$, $\Lambda_{vv'}^{3\mathcal{X}\mathcal{Y}} \equiv \lambda_{v33}^{\mathcal{X}*} \lambda_{v23}^{\mathcal{X}} \lambda_{v'33}^{\mathcal{Y}} \lambda_{v'23}^{\mathcal{Y}*}$, and $\Lambda_{vv'}^{4\mathcal{X}\mathcal{Y}} \equiv \lambda_{v33}^{\mathcal{X}} \lambda_{v23}^{\mathcal{X}*} \lambda_{v'33}^{\mathcal{Y}*} \lambda_{v'23}^{\mathcal{Y}}$ with \mathcal{X}, \mathcal{Y} being \mathcal{I} or \mathcal{R} , and $\Lambda_{vv'}^{\mathcal{N}} \equiv \lambda_{v33}^{\mathcal{N}} \lambda_{v23}^{\mathcal{N}*} \lambda_{v'33}^{\mathcal{N}} \lambda_{v'23}^{\mathcal{N}*}$. The formulas of Passarino-Veltman functions [68], D_0 and D_2 , are defined as

$$\begin{aligned} D_0[m_1, m_2, m_3, m_4] &\equiv \int \frac{d^4 k}{(2\pi)^4} \frac{1}{(k^2 - m_1^2)(k^2 - m_2^2)(k^2 - m_3^2)(k^2 - m_4^2)}, \\ D_2[m_1, m_2, m_3, m_4] &\equiv \int \frac{d^4 k}{(2\pi)^4} \frac{k^2}{(k^2 - m_1^2)(k^2 - m_2^2)(k^2 - m_3^2)(k^2 - m_4^2)}, \end{aligned} \quad (3.6)$$

and D_1 is given by $D_\mu = p_{i\mu} D_i$ [69], which is defined as

$$D_\mu \equiv \int \frac{d^4 k}{(2\pi)^4} \frac{k_\mu}{(k^2 - m_1^2)((k+p_1)^2 - m_2^2)((k+p_2)^2 - m_3^2)((k+p_3)^2 - m_4^2)}, \quad (3.7)$$

with the limit $p_i \cdot p_j \rightarrow 0$ applied. The chiral-flip contributions are all contained in the coefficient $C_{\text{NP}}^{\text{1SRR}}$, where the last two terms are extracted from the tree-level diagram. Combined with recent results of bag parameters, $B_s^{(i)}(m_b)$, including the new value of $B_s^{(1)}(m_b)$ [70, 71], we get the ratio,

$$\mathcal{R}_{B_s} \equiv \frac{\Delta M_s}{\Delta M_s^{\text{SM}}} = \left| 1 + \frac{C_{\text{NP}}^{\text{VLL}}}{C_{\text{SM}}^{\text{VLL}}} - 2.38 \frac{C_{\text{NP}}^{\text{1SRR}}}{C_{\text{SM}}^{\text{VLL}}} \right|. \quad (3.8)$$

The recent result averaged by the Heavy Flavor Averaging Group (HFLAV), $\Delta M_s^{\text{exp}} = (17.765 \pm 0.006) \text{ ps}^{-1}$ [72], along with the SM prediction $\Delta M_s^{\text{SM}} = (18.23 \pm 0.63) \text{ ps}^{-1}$ [73], leads to the strong constraint $0.90 < \mathcal{R}_{B_s} < 1.04$ at 2σ level. Given that the mass splitting of sneutrinos is considered in this work, the tree-level contributions to the ratio \mathcal{R}_{B_s} need the cancellation to fulfill the bound.

Next we investigate the cLFV processes, i.e. $\tau \rightarrow \ell\gamma$, $\mu \rightarrow e\gamma$, $\tau \rightarrow \ell'(\ell)\ell\ell$ ($\ell' \neq \ell$) and $\mu \rightarrow eee$. It should be stressed that the NP contributions from neutrino part, can be eliminated with the particular structures of (s)neutrino mass matrices. We utilize the structures where only chiral mixing but no flavor mixing exists for the neutrino sector involving RH neutrinos, as well as the whole sneutrino sector (see detailed discussions in Ref. [14] and appendix A). Then, we focus on the λ' contributions. The branching fraction of the $\tau \rightarrow \ell\gamma$ decay is given by [74]

$$\mathcal{B}(\tau \rightarrow \ell\gamma) = \frac{\tau_\tau \alpha m_\tau^5}{4} (|A_2^L|^2 + |A_2^R|^2), \quad (3.9)$$

where the effective couplings $A_2^L = -\lambda'_{\ell j 3} \lambda_{3 j 3}^* / 64\pi^2 m_{b_R}^2$ and $A_2^R = 0$, with the limit of $m_\ell^2/m_\tau^2 \rightarrow 0$ adopted here as well as the other cLFV processes. Because λ'_{2jk} is already set negligible, processes $\mu \rightarrow e\gamma$, $\mu \rightarrow eee$, $\tau \rightarrow \mu\gamma$, $\tau \rightarrow \mu\mu\mu$, and $\tau \rightarrow \ell'\ell\ell$, will not make effective bounds. Then the remaining ones to be considered are $\tau \rightarrow e\gamma$ and $\tau \rightarrow eee$ decays (see the relevant formulas in Ref. [59]), with the experimental upper limits $\mathcal{B}(\tau \rightarrow e\gamma)_{\text{exp}} < 3.3 \times 10^{-8}$ and $\mathcal{B}(\tau \rightarrow eee)_{\text{exp}} < 2.7 \times 10^{-8}$ at 90% CL, respectively [56].

Following the introduction of cLFV, we will mention the $B \rightarrow X_s\gamma$ decay, which are mastered by the electromagnetic dipole $C_{7\gamma s} \approx -C_{8gs}/3$ as well as C_{8gs} . Although the recent SM prediction $\mathcal{B}(B \rightarrow X_s\gamma)_{\text{SM}} \times 10^4 = 3.40 \pm 0.17$ ($E_\gamma > 1.6$ GeV) [75], agrees very well with the recent measured branching ratio $\mathcal{B}(B \rightarrow X_s\gamma)_{\text{exp}} \times 10^4 = 3.32 \pm 0.15$ [76], which implies a very strict constraint, both contributions to this branching ratio from $C_{7\gamma s}$ and C_{8gs} can counteract each other partly, shown as $\mathcal{B}(B \rightarrow X_s\gamma) \times 10^4 = (3.40 \pm 0.17) - 8.25 C_{7\gamma s}(\mu_{\text{EW}}) - 2.10 C_{8gs}(\mu_{\text{EW}})$ [75], so RPV-MSSMIS can avoid this stringent bound, given the value of $C_{8gs}(\mu_{\text{EW}})$ is expected around -0.1 (inducing $C_{7\gamma s}(\mu_{\text{EW}}) \approx 0.03$) for explaining non-leptonic puzzle.

In the following, we move on to the purely leptonic decays of Z , W bosons. The effective Lagrangian of Z -boson interaction to generic fermions $f_{i,j}$ is given by [77]

$$\mathcal{L}_{\text{eff}}^{Zff} = \frac{e}{\cos\theta_W \sin\theta_W} \bar{f}_i \gamma^\mu (g_{f_L}^{ij} P_L + g_{f_R}^{ij} P_R) f_j Z_\mu, \quad (3.10)$$

where $g_{f_L}^{ij} = \delta^{ij} g_{f_L}^{\text{SM}} + \delta g_{f_L}^{ij}$ and $g_{f_R}^{ij} = \delta^{ij} g_{f_R}^{\text{SM}} + \delta g_{f_R}^{ij}$. We first investigate $Z \rightarrow l_i^- l_j^+$ decay, and the relevant couplings, $g_{l_L}^{\text{SM}} = -\frac{1}{2} + \sin^2\theta_W$ and $g_{l_R}^{\text{SM}} = \sin^2\theta_W$. In the limit of $m_{l_i}/m_Z \rightarrow 0$,

the corresponding branching fractions are

$$\mathcal{B}(Z \rightarrow l_i^- l_j^+) = \frac{m_Z^3}{6\pi v^2 \Gamma_Z} (|g_{l_L}^{ij}|^2 + |g_{l_R}^{ij}|^2), \quad (3.11)$$

with Z -width $\Gamma_Z = 2.4955$ GeV [56]. For $i \neq j$, the branching ratio should be given by $[\mathcal{B}(Z \rightarrow l_i^- l_j^+) + \mathcal{B}(Z \rightarrow l_j^- l_i^+)]/2$. The NP effective couplings, contributed mainly by λ' effects, are expressed as $\delta g_{l_L}^{ij} = \frac{1}{32\pi^2} B^{ij}$ ($\delta g_{l_R}^{ij} = 0$) here and the formulas of B^{ij} functions are given by [58],

$$\begin{aligned} B_1^{ij} &= 3\tilde{\lambda}'_{j33}\tilde{\lambda}_{i33}^* \left\{ -x_{\tilde{b}_R}(1 + \log x_{\tilde{b}_R}) + \frac{m_Z^2}{18m_{\tilde{b}_R}^2} \left[(11 - 10\sin^2 \theta_W) \right. \right. \\ &\quad \left. \left. + (6 - 8\sin^2 \theta_W) \log x_{\tilde{b}_R} + \frac{1}{10}(-9 + 16\sin^2 \theta_W) \frac{m_Z^2}{m_t^2} \right] \right\}, \\ B_2^{ij} &= \sum_{\ell=1}^2 \tilde{\lambda}'_{j\ell 3} \tilde{\lambda}_{i\ell 3}^* \frac{m_Z^2}{m_{\tilde{b}_R}^2} \left[\left(1 - \frac{4}{3}\sin^2 \theta_W\right) \left(\log \frac{m_Z^2}{m_{\tilde{b}_R}^2} - i\pi - \frac{1}{3}\right) + \frac{\sin^2 \theta_W}{9} \right]. \end{aligned} \quad (3.12)$$

With the data of the partial width ratios of Z bosons, i.e. $\Gamma(Z \rightarrow \mu\mu)/\Gamma(Z \rightarrow ee) = 1.0001(24)$, $\Gamma(Z \rightarrow \tau\tau)/\Gamma(Z \rightarrow \mu\mu) = 1.0010(26)$ and $\Gamma(Z \rightarrow \tau\tau)/\Gamma(Z \rightarrow ee) = 1.0020(32)$ [56], we have the bound of $|B^{11}| < 0.36$ with $|B^{33}| < 0.32$. And the upper limit of the branching ratio, $B(Z \rightarrow e\tau) < 9.8 \times 10^{-6}$ at 95% CL [56], makes the bound $|B^{13}|^2 + |B^{31}|^2 < 1.4^2$.

Then we study the invisible Z -decays, i.e. Z boson interaction to neutrinos, mainly in this model. The effective number of light neutrinos N_ν , defined by $\Gamma_{\text{inv}} = N_\nu \Gamma_{\nu\bar{\nu}}^{\text{SM}}$ [78], will constrain the relevant couplings g_ν in Eq. (3.10), via

$$N_\nu = \sum_{i,j} \left| \delta_{ij} + \frac{\delta g_\nu^{ij}}{\delta g_\nu^{\text{SM}}} \right|^2, \quad (3.13)$$

where the coupling $\delta g_\nu^{\text{SM}} = \frac{1}{2}$ and the formula of δg_ν^{ij} is given by [79]

$$(32\pi^2)\delta g_\nu^{ij} = \lambda'_{j33}\lambda_{i33}^* \frac{m_Z^2}{m_{\tilde{b}_R}^2} \left\{ \left(-1 + \frac{2}{3}\sin^2 \theta_W\right) \left[\log \left(\frac{m_Z^2}{m_{\tilde{b}_R}^2} \right) - i\pi - \frac{1}{3} \right] + \left(-\frac{1}{12} + \frac{4}{9}\sin^2 \theta_W\right) \right\}. \quad (3.14)$$

Then the measurement result $N_\nu^{\text{exp}} = 2.9840(82)$ [78] will make constraints.

As for the purely leptonic decays of the W boson, they can be covered by the stronger ones from $\mu \rightarrow e\bar{\nu}_e\nu_\mu$ and $\tau \rightarrow \ell\bar{\nu}_\ell\nu_\tau$ decays. The fraction ratios of these lepton decays, i.e.

$\mathcal{B}(\tau \rightarrow \mu \bar{\nu}_\mu \nu_\tau)/\mathcal{B}(\tau \rightarrow e \bar{\nu}_e \nu_\tau)$, $\mathcal{B}(\tau \rightarrow e \bar{\nu}_e \nu_\tau)/\mathcal{B}(\mu \rightarrow e \bar{\nu}_e \nu_\mu)$ and $\mathcal{B}(\tau \rightarrow \mu \bar{\nu}_\mu \nu_\tau)/\mathcal{B}(\mu \rightarrow e \bar{\nu}_e \nu_\mu)$, make the bounds [60] on the model parameters, which can be expressed as

$$\begin{aligned}\frac{1 + \eta_{\mu\mu}}{1 + \eta_{ee} + h'_{ee}} &= 1.0018(14), \\ \frac{1 + \eta_{\tau\tau} + h'_{\tau\tau}}{1 + \eta_{\mu\mu}} &= 1.0010(14), \\ \frac{1 + \eta_{\tau\tau} + h'_{\tau\tau}}{1 + \eta_{ee} + h'_{ee}} &= 1.0029(14).\end{aligned}\tag{3.15}$$

Here we only consider the $Wl\nu_l$ vertex, which has the interference with the SM contribution, and the LFV vertexes $Wl\nu_{l'}$ and Zll' , which can be embedded in $l \rightarrow l' \bar{\nu}_i \nu_j$ process, are omitted. With the last two formulas of Eq. (3.15) combined with $|\eta_{\mu\mu}| \lesssim 10^{-4}$, we should keep $|\eta_{\tau\tau} + h'_{\tau\tau}| \lesssim 0.0018$ and $|\eta_{\tau\tau} + h'_{\tau\tau}| \lesssim |\eta_{ee} + h'_{ee}|$ at 2σ level.

One knows that the η and h' functions in Eq. (3.15) also affect the W -boson mass predictions, $m_W^{\text{NP}} \approx m_W^{\text{SM}}[1 - 0.20(\eta_{ee} + \eta_{\mu\mu} + h'_{ee})]$ [80], through $G_\mu = G_F(1 + \eta_{\ell\ell} + h'_{\ell\ell})$ [60, 62], where G_μ is the Fermi constant extracted from the muon lifetime, while G_F corresponds to the one in the SM. Here we omit the contributions of oblique parameters, i.e. S , T , and U , from the self-energy of gauge bosons. In the following, we will illustrate the reason. The one-loop contributions to the oblique parameters in RPV-MSSMIS can be divided into the MSSM part and seesaw part, and obviously, there are no λ' couplings engaging the boson self-energy diagrams at one-loop level. The MSSM part is dominated by the one-loop diagrams involving pure squarks [81] and the seesaw part is dominated by the one involving light leptons combined with heavy neutrinos [44]. First we utilize **SPheno** [82, 83] code, generated by package **SARAH**, to calculate oblique parameters of MSSM part with inputs in table 2 and the benchmark points we in table 3 in the following section. The results show that S , T , and U from the MSSM part all stay less than 10^{-4} and can be omitted safely. As for the seesaw-part, the recent research shows that this bound is weaker than the one from the decays $Z \rightarrow \ell\tau$ and the invisible Z - decays [44], which are discussed before in this section. To summarize, the constraints from the oblique parameters can be accord with the explanation for the non-leptonic puzzle in this work.

At last, we scrutinize all the one-loop level diagrams of $b \rightarrow s \ell^+ \ell^-$ to search for the potential chiral-flip contributions. Here we use the same definitions of semi-leptonic coefficients in our recent work [15], i.e. $C_9^{\text{NP}} = C_{9e}^{\text{NP}} + C_{9U}^{\text{NP}}$ and $C_{10}^{\text{NP}} = C_{10e}^{\text{NP}} + C_{10U}^{\text{NP}}$, where $C_{9(10)e}^{\text{NP}}$ express the lepton flavor non-universal contributions while $C_{9(10)U}^{\text{NP}}$ express the lepton flavor universal ones. Under the ‘‘single-value- k ’’ assumption stated in Sec. 2, we find that there exist $C_{9e}^{\text{NP}} = -C_{10e}^{\text{NP}}$

Parameters	Sets	Parameters	Sets
$\tan \beta$	5	$M_{\tilde{Q}_i}$	10 TeV
Y_ν	diag(0.28, 0.11, 0.10)	$M_{\tilde{U}_i}$	5 TeV
M_{R_i}	1 TeV	$m_{\tilde{L}_i}$	1 TeV
$B_{M_{R_i}}$	0.5 TeV ²	$M_{\tilde{E}_i}$	2 TeV
$B_{\mu_{S_i}}$	-0.66 TeV ²	m_A	2 TeV
A_{ν_i}	2.4 TeV	A_t	-4 TeV

Table 2: The sets of fixed parameters of RPV-MSSMIS.

as well as $C_{10U}^{\text{NP}} = 0$, the same as the ones of degenerate-mass scenario [14].

4 Numerical analyses

In this section, we begin to analyse $B_{d(s)} \rightarrow K^{(*)} \bar{K}^{(*)}$ and $B \rightarrow K^{(*)} \nu \bar{\nu}$ numerically within the mass-splitting scenario of RPV-MSSMIS. We consider normal ordering and $\delta_{\text{CP}} = \pi$ with the recent data of neutrino oscillation [84, 85]. Then it can be calculated that the three light neutrinos have masses $\{0, 0.008, 0.05\}$ eV with $m_{\nu_i} \approx \{0, \sqrt{\Delta m_{21}^2}, \sqrt{\Delta m_{31}^2}\}$ [86]. We set $\tan \beta = 5$ as the benchmark, which provides the larger room for the mass of CP-odd Higgs considering the LHC bounds [87–89]. All the sets of fixed model parameters are collected in table 2.

The diagonal inputs of Y_ν , M_R , $m_{\tilde{L}'}$, B_{M_R} , and B_{μ_S} here can induce no flavor mixings in sneutrino sector, as well as the neutrino sector which RH neutrinos engage in, and this is benefit for fulfilling the bounds of cLFV decays. Besides, the input values shown in table 2 can induce a diagonal $\eta = -\text{diag}(1.18, 0.18, 0.15) \times 10^{-3}$, which induces the W mass prediction $M_W \approx 80.385$ GeV, fulfilling the recent data [56]. The values of $m_{\tilde{L}'}$ induce physical mass of the lightest sneutrino, as $m_{\tilde{\nu}_1} \approx 270$ GeV, allowed by the relevant constraints [56] (non- λ and decoupled-chargino case), while the masses of charged sleptons are not affected by B_{μ_S} and they are predicted as TeV scale, which in accord with the ATLAS results discussed in section 3.2. The remaining parameters, i.e. $m_{\tilde{b}_R}$, λ'_{323} , λ'_{333} , λ'_{123} and λ'_{133} , can vary freely in the ranges considered.

With the inputs given above, we can get the numerical results of the Wilson coefficient and

observable, which contain chiral-flip effects, as follows,

$$C_{8gs}^{\text{NP}} = (0.027 + P(m_{\tilde{b}_R}))\lambda_{123}'^*\lambda_{133}' + 0.004\lambda_{323}'^*\lambda_{333}' + 0.061\lambda_{123}'^*\lambda_{133}' + 0.062\lambda_{323}'^*\lambda_{333}',$$

$$\mathcal{R}_{B_s} \approx \left| 1 + 156.04\lambda_{123}'^{*2} + 21.59\lambda_{323}'^{*2} + B(m_{\tilde{b}_R}) (\lambda_{123}'^*\lambda_{133}' + \lambda_{323}'^*\lambda_{333}')^2 \right|, \quad (4.1)$$

where the parameters $P(m_{\tilde{b}_R})$ and $B(m_{\tilde{b}_R})$ represent the contributions from penguin diagrams involving \tilde{b}_R and box ones involving both \tilde{b}_R and $\tilde{\nu}$. In Eq. (4.1), ones can see that cancellations are preferred in both the chiral-flip term $156.04\lambda_{123}'^{*2} + 21.59\lambda_{323}'^{*2}$ and the non-flip one $\lambda_{123}'^*\lambda_{133}' + \lambda_{323}'^*\lambda_{333}'$, because of the stringent constraints of B_s - \bar{B}_s mixing. The chiral-flip term demands for a tuning relation between λ_{123}' and λ_{323}' , so at least, one of them should be imaginary. In the following, we set that $\lambda_{123}' = r\lambda_{323}'i$ ($r = (\frac{21.59}{156.04})^{\frac{1}{2}} \approx 0.3719$ throughout this paper), and accordingly, the coupling λ_{133}' is also set imaginary and approaching $-i\lambda_{333}'/r$, while couplings λ_{323}' and λ_{333}' are set real. Thus, ones can see that $|\lambda_{133}'|$ and $|\lambda_{323}'|$ are the larger ones among these $|\lambda'|$ values.

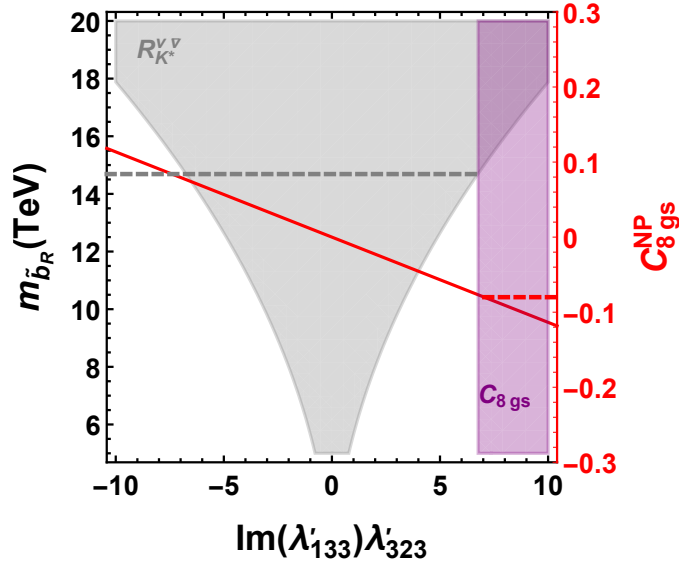


Figure 2: The 2σ -level favored regions of $(\text{Im}(\lambda'_{133})\lambda'_{323}, m_{\tilde{b}_R})$ for explaining the $B_{d(s)} \rightarrow K^{(*)}\bar{K}^{(*)}$ puzzle (purple region), with regions allowed by the $B \rightarrow K^*\nu\bar{\nu}$ data at 2σ level (gray region), combined with the Wilson coefficient C_{8gs}^{NP} varying with $\text{Im}(\lambda'_{133})\lambda'_{323}$, expressed by the solid red line. In this figure, both $\lambda'_{123} = r\lambda'_{323}i$ and $\lambda'_{333} = -r\text{Im}(\lambda'_{133})$ are set.

Therefore, the Wilson coefficient C_{8gs}^{NP} , which is critical for the $B_{d(s)} \rightarrow K^{(*)}\bar{K}^{(*)}$ puzzle, is dominated by $-[0.01 + 0.37P(m_{\tilde{b}_R})]\text{Im}(\lambda'_{133})\lambda'_{323}$. Given we calculate that $P(m_{\tilde{b}_R}) \lesssim 10^{-3}$ for

$m_{\tilde{b}_R} \gtrsim 1$ TeV, we can further get $C_{8gs}^{\text{NP}} \approx -0.01 \text{Im}(\lambda'_{133})\lambda'_{323}$. Then, with the set, $\lambda'_{123} = r\lambda'_{323}i$ and $\lambda'_{333} = -r\text{Im}(\lambda'_{133})$, we can get,

$$\begin{aligned} R_{K^{(*)}}^{\nu\bar{\nu}} \approx & 653X_{\tilde{b}_R}^2 + 0.29 \left| 1.07 - 8.78X_{\tilde{b}_R} - (0.02 + 6.06X_{\tilde{b}_R})i \right|^2 \\ & + 0.29 \left| 1.07 - 0.44X_{\tilde{b}_R} - (0.02 + 15.66X_{\tilde{b}_R})i \right|^2 \\ & + 0.29 \left| 1.07 + 9.18X_{\tilde{b}_R} - (0.02 - 21.72X_{\tilde{b}_R})i \right|^2, \end{aligned} \quad (4.2)$$

where the real-number function $X_{\tilde{b}_R} = \text{Im}(\lambda'_{133})\lambda'_{323}/(m_{\tilde{b}_R}/\text{TeV})^2$. In Fig. 2, we show the common region for non-leptonic puzzle explanation and $B \rightarrow K^*\nu\bar{\nu}$ data, and find that $\text{Im}(\lambda'_{133})\lambda'_{323} \gtrsim 6.8$ should be fulfilled to explain the puzzle, which induces $m_{\tilde{b}_R}$ above around 15 TeV to below the up limit of $\mathcal{B}(B \rightarrow K^*\nu\bar{\nu})_{\text{exp}}$. As shown above, even when the sbottom reach 10 TeV scale, $R_K^{\nu\bar{\nu}}$ can still be close to 1.9, provided both $|\lambda'_{133}|$ and $|\lambda'_{323}|$ are sufficiently large. However, this case will not make non-negligible effects on the $b \rightarrow s e \tau$ process, because the exchanging squark of its tree diagram is up type instead, not accord with the single-value- k assumption (λ'_{i32} engaged). As for one-loop level, the relevant NP contributions are dominated by $4\lambda'$ boxes, given by [14],

$$\begin{aligned} \Delta C_{9e\tau}^{4\lambda'} = -\Delta C_{10e\tau}^{4\lambda'} = & -\frac{\sqrt{2}\pi^2 i}{2G_F\eta_t e^2} \left(\tilde{\lambda}'_{1i3} \tilde{\lambda}'_{3i3}^* \lambda'_{v33} \lambda'_{v23} D_2[m_{\nu_v}, m_{u_i}, m_{\tilde{b}_R}, m_{\tilde{b}_R}] \right. \\ & \left. + \tilde{\lambda}'_{1i3} \tilde{\lambda}'_{3i3}^* \lambda'_{v33} \lambda'_{v23} D_2[m_{\tilde{\nu}_v^T}, m_{\tilde{u}_{Li}}, m_b, m_b] \right). \end{aligned} \quad (4.3)$$

Due to the cancellation in $\lambda'_{123}\lambda'_{133} + \lambda'_{323}\lambda'_{333}$, this loop contribution is also suppressed. Besides, as mentioned in Sec. 2.2, there also contain chiral-flip effects in the result of C_{9U}^{NP} , without the logarithmic enhancement. We find that C_{9U}^{NP} as well as $C_{9e}^{\text{NP}} = -C_{10e}^{\text{NP}}$, can be up to $\mathcal{O}(10^{-2})$ in the allowed parameter space. However, the chiral-flip contributions are negligible. We also check the charged processes $d_j \rightarrow u_n l \nu$, and among them, only $b \rightarrow c \tau \nu_e$ transition is affected by large $(|\lambda'_{133}|, |\lambda'_{323}|)$. Utilizing Eq. (2.11) in Ref. [15], we find the related NP contribution versus SM one is about $\mathcal{O}(10^{-3})$ scale, which is negligible.

With the rough NP features above, next, we move onto the concrete numerical analysis. As shown in Fig. 3, ones can see that the $B_{d(s)} \rightarrow K^{(*)}\bar{K}^{(*)}$ puzzle can be explained in RPV-MSSMIS, at 2σ level. The $\tau \rightarrow eee$ decay, $B_s - \bar{B}_s$ mixing, and $B \rightarrow K^*\nu\bar{\nu}$ decay, provide the dominant constraints, and the perturbativity limit is also shown. In Fig. 3a, λ'_{123} and λ'_{133} are set related to λ'_{323} and λ'_{333} , respectively, and $m_{\tilde{b}_R}$ is 18 TeV. The process bounds on λ'_{333}

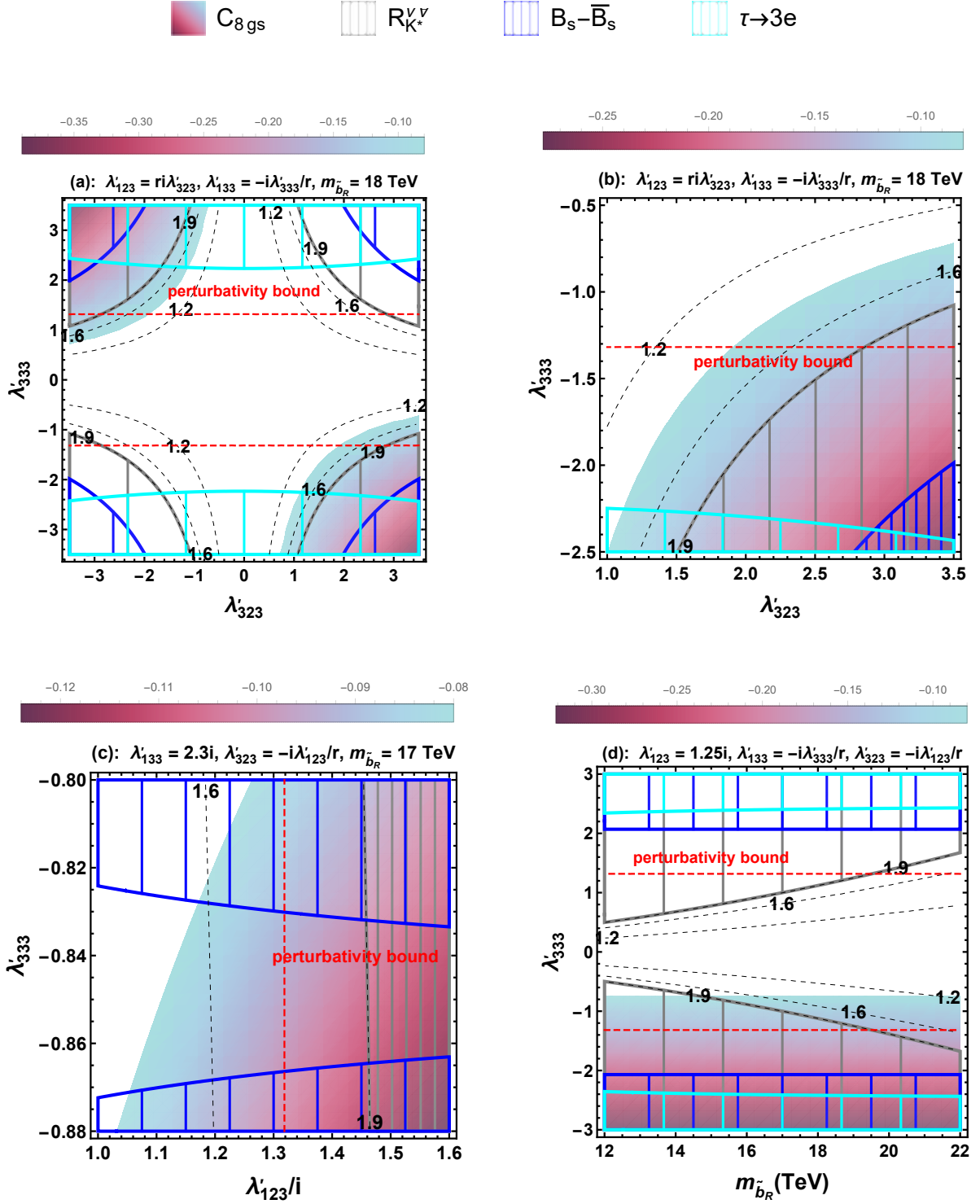


Figure 3: The 2σ -level allowed regions for explaining the $B_{d(s)} \rightarrow K^{(*)} \bar{K}^{(*)}$ puzzle. The favored areas for the non-leptonic puzzle explanation is denoted by a colored gradient, where the negative coefficient C_{8gs}^{NP} approaches the lower (higher) value when points approaching the red (blue) area. The black dashed lines express the values of $R_{K^{(*)}}^{\nu\bar{\nu}}$. The hatched areas filled with the cyan, blue and gray lines are excluded by the $\tau \rightarrow eee$ decays, $B_s - \bar{B}_s$ mixing, and $B \rightarrow K^* \nu \bar{\nu}$, respectively. The red dashed lines express the perturbativity limit, i.e. any $|\lambda'| \leq \sqrt{4\pi}$.

are mainly $\tau \rightarrow eee$ and $B \rightarrow K^* \nu \bar{\nu}$ decays, while nearly overlapped by the exclusion area of perturbativity bound. With the same set, Fig. 3b shows the common region in detail, which shows that λ'_{323} should be larger than around 2.3. And λ'_{333} should be about lower than -0.7 and also higher than -1.3 . In Fig. 3c, we set $\lambda'_{133} = 2.3i$, and then, the ranges for puzzle explanation are $1.02 \lesssim \text{Im}(\lambda'_{123}) \lesssim 1.29$ and $-0.87 \lesssim \lambda'_{333} \lesssim -0.83$. In Fig. 3d, λ'_{123} is set as $1.25i$, ones can see that the ratios $R_{K^{(*)}}^{\nu\bar{\nu}}$ increase with sbottom mass increasing for $\lambda'_{333} > 0$, while decrease with sbottom mass increasing for $\lambda'_{333} < 0$. The puzzle explanation favors $-1.29 \lesssim \lambda'_{333} \lesssim -0.8$ and $m_{\tilde{b}_R} \gtrsim 15$ TeV.

$m_{\tilde{b}_R}$	λ'_{123}	λ'_{133}	λ'_{323}	λ'_{333}	$R_{K^{(*)}}^{\nu\bar{\nu}}$	C_{8gs}^{NP}	$L_{K\bar{K}}$	$L_{K^*\bar{K}^*}$	$\mathcal{B}_{VP} \times 10^5$
17 TeV	$1.2i$	$2.3i$	3.23	-0.84	1.61	-0.084	23.58	15.80	0.80
19 TeV	$1.1i$	$2.8i$	2.96	-1.04	1.48	-0.098	23.21	15.26	0.79
21 TeV	$1.1i$	$3.0i$	2.96	-1.1	1.37	-0.102	23.10	15.09	0.79

Table 3: The benchmark points favored by the puzzle explanation. Here \mathcal{B}_{VP} is the untagged branching ratio $\mathcal{B}(\bar{B}_s \rightarrow K^{*0} \bar{K}^0 + c.c.)$.

Afterwards, we collect some benchmark points in table 3 where the pseudoscalar-vector channel is also calculated. We consider the untagged transition $\bar{B}_s \rightarrow K^{*0} \bar{K}^0$ with the branching ratio measured as $\mathcal{B}(\bar{B}_s \rightarrow K^{*0} \bar{K}^0 + c.c.)_{\text{exp}} = (1.98 \pm 0.28 \pm 0.50) \times 10^{-5}$ [90]. With the Wilson coefficient $C_{8gs}^{\text{NP}}(\mu_{\text{EW}})$, ones can predict this branching ratio in NP [12],

$$\mathcal{B}(\bar{B}_s \rightarrow K^{*0} \bar{K}^0 + c.c.) \times 10^5 = 0.87 + 0.87 C_{8gs}^{\text{NP}}(\mu_{\text{EW}}) + 0.95 C_{8gs}^{\text{NP}}(\mu_{\text{EW}})^2. \quad (4.4)$$

5 Additional remarks

Before we conclude this work, it is worth having a discussion on whether the imaginary λ' couplings may affect CP violations. Firstly we check the NP CPV in the $B_s - \bar{B}_s$ mixing. Given the formulas of Wilson coefficients shown in Eq. (3.5), along with flavor non-mixings in sneutrino content, the extra imaginary part, i.e. NP CPV not from CKM, can be only from the term, $\Lambda_{vv'}^{\mathcal{N}} D_2[m_{\nu_v}, m_{\nu_{v'}}, m_{\tilde{b}_R}, m_{\tilde{b}_R}]$, containing factor $\lambda'_{133} \lambda'_{323} \mathcal{V}_{v(\prime)1} \mathcal{V}_{v(\prime)3}^*$. However, $\mathcal{V}_{v(\prime)1} \mathcal{V}_{v(\prime)3}^*$ for light-neutrino content provides suppressing effects due to the unitarity of PMNS. In concrete numerical calculations, we confirm that this imaginary contribution can be omitted.

Next we examine the potential CPV from Z boson partial decay, which are proportional to ratios of the coupling constants, $\text{Im}(\lambda'_{iJ3} \lambda'_{iJ3} / \lambda'_{1J3} \lambda'_{1J3})$ [91]. Given we set λ'_{123} and λ'_{133} both

purely imaginary, while λ'_{323} and λ'_{333} both real, these ratios have no imaginary part.

At last, we move onto the electron electric dipole moment (EDM), related to a $u\tilde{d}\tilde{d}$ -loop in the $ee\gamma$ diagram, that is proportional to the factor $[(\cos^2 \beta_{\lambda'_{1jk}} - \sin^2 \beta_{\lambda'_{1jk}}) \sin \alpha_{A_d} + \cos \beta_{\lambda'_{1jk}} \sin \beta_{\lambda'_{1jk}} \cos \alpha_{A_d}][|\lambda'_{1jk}|^2]$ [92], where the α_{A_d} and $\beta_{\lambda'_{1jk}}$ are the related arguments. In the scenario of this work, we have $\beta_{\lambda'_{1jk}} = \pi/2$. With a suppressed non-positive α_{A_d} , the constraint from electron EDM can be fulfilled. As for neutron EDMs, we should consider the $uu\gamma$ and $dd\gamma$ diagrams at one-loop level, where the $uu\gamma$ diagram always contains the λ'_{i1k} couplings and the $dd\gamma$ diagram always contains the λ'_{i1k} or λ'_{ij1} couplings. Even when further considering two-loop contributions, e.g. Barr-Zee type, the result still contains these couplings [93]. Besides, the bounds from EDMs of several nuclei and atoms, still involve λ'_{ij1} as well as additional λ'_{ij2} [94]. Given that both λ'_{i1k} and $\lambda'_{ij1(2)}$ are already set negligible in this work, the bounds of hadronic EDMs can be fulfilled safely.

6 Conclusions

The recent measurements of $B_{d(s)} \rightarrow K^{(*)} \bar{K}^{(*)}$ show a non-leptonic puzzle, which expresses the deviations between the data and the QCD-factorisation prediction for the U-spin related observable, $L_{K^{(*)} \bar{K}^{(*)}}$. Besides, Belle II has recently reported the new measurement of $\mathcal{B}(B^+ \rightarrow K^+ \nu \bar{\nu})$, around 2.7σ above the SM prediction. Both of the tensions imply that, there may exist new quark-flavor structure beyond the SM.

In this work, we study the non-leptonic puzzle and $B^+ \rightarrow K^+ \nu \bar{\nu}$ in RPV-MSSMIS. This NP framework connects the trilinear interaction $\lambda' \hat{L} \hat{Q} \hat{D}$ with the (s)neutrino chirality flip to make the unique contribution to $L_{K^{(*)} \bar{K}^{(*)}}$, through the gluon-penguin diagrams. The chiral-flip effects are expressed as the double- λ' terms in the Wilson coefficient $C_{8gs,d}^{\text{NP}}$, which can be enhanced by the logarithm and explain the related deviation. In the $B_s - \bar{B}_s$ mixing, there also exist chiral-flip contributions, and to fulfill the strict bound of experimental data, the scenario of imaginary λ'_{123} , λ'_{133} with real λ'_{323} , λ'_{333} is adopted. The effect on the CPV due to this scenario is investigated as well. As for $B^+ \rightarrow K^+ \nu \bar{\nu}$ decays, we find that the large $|\lambda'_{133}|$ and $|\lambda'_{323}|$, can make some enhancements, even when sbottoms are as heavy as 10 TeV. At last, we provide some benchmark points, which also fulfill collider bounds, neutrino data, and series of flavor-physics constraints from B, K -semileptonic decays, Z decays, cLFV processes, etc.

Acknowledgements

M.D. thanks Xing-Bo Yuan for valuable discussions. This work is supported in part by Jiangxi Province Key Laboratory of Applied Optical Technology (Grant No. 2024SSY03051), the National Natural Science Foundation of China under Grant No. 12275367, the Fundamental Research Funds for the Central Universities, and the Sun Yat-Sen University Science Foundation.

A The numerical form of the (s)neutrino mixing matrix

With the input set in table 2, the numerical form of the neutrino mixing matrix is listed as

$$\mathcal{V}^T \approx \begin{pmatrix} 0.842 & 0.516 & -0.152 & 0.034i & 0 & 0 & 0.034 & 0 & 0 \\ -0.283 & 0.665 & 0.690 & 0 & 0.013i & 0 & 0 & 0.013 & 0 \\ 0.458 & -0.538 & 0.707 & 0 & 0 & 0.012i & 0 & 0 & 0.012 \\ 0 & 0 & 0 & -0.707i & 0 & 0 & 0.707 & 0 & 0 \\ 0 & 0 & 0 & 0 & -0.707i & 0 & 0 & 0.707 & 0 \\ 0 & 0 & 0 & 0 & 0 & -0.707i & 0 & 0 & 0.707 \\ -0.040 & -0.025 & 0.007 & 0.706i & 0 & 0 & 0.706 & 0 & 0 \\ 0.005 & -0.012 & -0.013 & 0 & 0.707i & 0 & 0 & 0.707 & 0 \\ -0.008 & 0.009 & -0.012 & 0 & 0 & 0.707i & 0 & 0 & 0.707 \end{pmatrix}, \quad (\text{A.1})$$

which is related to the neutrino mass spectrum around $\{0, 8 \times 10^{-15}, 5 \times 10^{-14}, 1, 1, 1, 1, 1, 1\}$ TeV. And the sneutrino mixing matrices are given numerically by

$$\tilde{\mathcal{V}}^{\mathcal{R}} \approx \begin{pmatrix} -0.044 & 0 & 0 & -0.473 & 0 & 0 & 0.880 & 0 & 0 \\ 0 & -0.018 & 0 & 0 & -0.475 & 0 & 0 & 0.880 & 0 \\ 0 & 0 & -0.016 & 0 & 0 & -0.475 & 0 & 0 & 0.880 \\ 0.995 & 0 & 0 & -0.100 & 0 & 0 & -0.004 & 0 & 0 \\ 0 & -0.999 & 0 & 0 & 0.038 & 0 & 0 & 0.001 & 0 \\ 0 & 0 & -0.999 & 0 & 0 & 0.034 & 0 & 0 & 0 \\ 0.089 & 0 & 0 & 0.875 & 0 & 0 & 0.475 & 0 & 0 \\ 0 & -0.034 & 0 & 0 & -0.879 & 0 & 0 & -0.475 & 0 \\ 0 & 0 & -0.030 & 0 & 0 & -0.879 & 0 & 0 & -0.475 \end{pmatrix}, \quad (\text{A.2})$$

related to the $m_{\tilde{\nu}^{\mathcal{R}}}$ spectrum $\{269, 272, 272, 1010, 1005, 1000, 1129, 1127, 1127\}$ GeV, as well as

$$\tilde{\mathcal{V}}^{\mathcal{I}} \approx \begin{pmatrix} -0.078 & 0 & 0 & -0.876 & 0 & 0 & 0.477 & 0 & 0 \\ 0 & -0.032 & 0 & 0 & -0.879 & 0 & 0 & 0.475 & 0 \\ 0 & 0 & -0.030 & 0 & 0 & -0.879 & 0 & 0 & 0.475 \\ -0.996 & 0 & 0 & 0.091 & 0 & 0 & 0.003 & 0 & 0 \\ 0 & 0.999 & 0 & 0 & -0.037 & 0 & 0 & -0.001 & 0 \\ 0 & 0 & -0.999 & 0 & 0 & 0.034 & 0 & 0 & 0 \\ 0.046 & 0 & 0 & 0.475 & 0 & 0 & 0.879 & 0 & 0 \\ 0 & 0.018 & 0 & 0 & 0.475 & 0 & 0 & 0.880 & 0 \\ 0 & 0 & 0.016 & 0 & 0 & 0.475 & 0 & 0 & 0.880 \end{pmatrix}, \quad (\text{A.3})$$

related to the $m_{\tilde{\nu}^{\mathcal{I}}}$ spectrum $\{854, 854, 854, 1010, 1005, 1000, 1389, 1388, 1388\}$ GeV.

Then ones can find, all the chargino-sneutrino diagrams and the neutralino-slepton diagrams, among the non- λ' diagrams in the cLFV decays of leptons, make negligible contributions due to the vanishing of flavor mixing in sneutrino sector, as shown in Eq. (A.2) and Eq. (A.3). As to W/H^\pm -neutrino diagrams, they are always connected to terms $\mathcal{V}_{(\alpha+3)v}^{T*} \mathcal{V}_{(\beta+3)v}^T$, $\mathcal{V}_{(\alpha+3)v}^{T*} \mathcal{V}_{\beta v}^T$, $\mathcal{V}_{\alpha v}^{T*} \mathcal{V}_{\beta v}^T$ and conjugate terms ($\alpha, \beta = e, \mu, \tau$ and $\alpha \neq \beta$). Readers can see calculations

of these diagrams in Ref. [95]. With the numerical form of Eq. (A.1), the $\mathcal{V}_{(\alpha+3)v}^{T*} \mathcal{V}_{(\beta+3)v}^T$ and $\mathcal{V}_{(\alpha+3)v}^{T*} \mathcal{V}_{\beta v}^T$ terms vanish. The $\mathcal{V}_{\alpha v}^{T*} \mathcal{V}_{\beta v}^T$ term can be decomposed into two parts, $\sum_{N=4}^9 \mathcal{V}_{\alpha N}^{T*} \mathcal{V}_{\beta N}^T$ and $\sum_{i=1}^3 \mathcal{V}_{\alpha i}^{T*} \mathcal{V}_{\beta i}^T = -\sum_{N=4}^9 \mathcal{V}_{\alpha N}^{T*} \mathcal{V}_{\beta N}^T$, related to the nearly degenerate heavy neutrinos and light neutrinos respectively [96]. Then ones can also find that the $\mathcal{V}_{\alpha v}^{T*} \mathcal{V}_{\beta v}^T$ term makes no effective contribution to the cLFV decays. Thus, we conclude that the non- λ' diagrams provide negligible effects on the cLFV decays, as mentioned in section 3.4, in our input sets.

References

- [1] **LHCb** Collaboration, R. Aaij et al., *Test of lepton universality in $b \rightarrow s \ell^+ \ell^-$ decays*, *Phys. Rev. Lett.* **131** (2023), no. 5 051803, [arXiv:2212.09152].
- [2] A. Biswas, S. Descotes-Genon, J. Matias, and G. Tetlalmatzi-Xolocotzi, *A new puzzle in non-leptonic B decays*, *JHEP* **06** (2023) 108, [arXiv:2301.10542].
- [3] **Particle Data Group** Collaboration, R. L. Workman et al., *Review of Particle Physics*, *PTEP* **2022** (2022) 083C01.
- [4] **BaBar** Collaboration, B. Aubert et al., *Observation of $B^0 \rightarrow K^{*0} \bar{K}^{*0}$ and search for $B^0 \rightarrow K^{*0} K^{*0}$* , *Phys. Rev. Lett.* **100** (2008) 081801, [arXiv:0708.2248].
- [5] **LHCb** Collaboration, R. Aaij et al., *Amplitude analysis of the $B_{(s)}^0 \rightarrow K^{*0} \bar{K}^{*0}$ decays and measurement of the branching fraction of the $B^0 \rightarrow K^{*0} \bar{K}^{*0}$ decay*, *JHEP* **07** (2019) 032, [arXiv:1905.06662].
- [6] **BaBar** Collaboration, B. Aubert et al., *Observation of $B^+ \rightarrow \bar{K}^0 K^+$ and $B^0 \rightarrow K^0 \bar{K}^0$* , *Phys. Rev. Lett.* **97** (2006) 171805, [hep-ex/0608036].
- [7] **Belle** Collaboration, Y. T. Duh et al., *Measurements of branching fractions and direct CP asymmetries for $B \rightarrow K\pi$, $B \rightarrow \pi\pi$ and $B \rightarrow KK$ decays*, *Phys. Rev. D* **87** (2013), no. 3 031103, [arXiv:1210.1348].
- [8] **Belle** Collaboration, B. Pal et al., *Observation of the decay $B_s^0 \rightarrow K^0 \bar{K}^0$* , *Phys. Rev. Lett.* **116** (2016), no. 16 161801, [arXiv:1512.02145].
- [9] **LHCb** Collaboration, R. Aaij et al., *Measurement of the branching fraction of the decay $B_s^0 \rightarrow K_S^0 K_S^0$* , *Phys. Rev. D* **102** (2020), no. 1 012011, [arXiv:2002.08229].

- [10] M. Beneke, G. Buchalla, M. Neubert, and C. T. Sachrajda, *QCD factorization in $B \rightarrow \pi K$, $\pi\pi$ decays and extraction of Wolfenstein parameters*, *Nucl. Phys. B* **606** (2001) 245–321, [[hep-ph/0104110](#)].
- [11] M. Algueró, A. Crivellin, S. Descotes-Genon, J. Matias, and M. Novoa-Brunet, *A new B -flavour anomaly in $B_{d,s} \rightarrow K^{*0} \bar{K}^{*0}$: anatomy and interpretation*, *JHEP* **04** (2021) 066, [[arXiv:2011.07867](#)].
- [12] A. Biswas, S. Descotes-Genon, J. Matias, and G. Tetlalmatzi-Xolocotzi, *Optimised observables and new physics prospects in the penguin-mediated decays $B_{d(s)} \rightarrow K^{(*)0} \phi$* , *JHEP* **08** (2024) 030, [[arXiv:2404.01186](#)].
- [13] J. M. Lizana, J. Matias, and B. A. Stefanek, *Explaining the $B_{d,s} \rightarrow K^{(*)} \bar{K}^{(*)}$ non-leptonic puzzle and charged-current B -anomalies via scalar leptoquarks*, *JHEP* **09** (2023) 114, [[arXiv:2306.09178](#)].
- [14] M.-D. Zheng and H.-H. Zhang, *Studying the $b \rightarrow s \ell^+ \ell^-$ anomalies and $(g - 2)_\mu$ in R -parity violating MSSM framework with the inverse seesaw mechanism*, *Phys. Rev. D* **104** (2021), no. 11 115023, [[arXiv:2105.06954](#)].
- [15] M.-D. Zheng, F.-Z. Chen, and H.-H. Zhang, *Explaining anomalies of B -physics, muon $g - 2$ and W mass in R -parity violating MSSM with seesaw mechanism*, *Eur. Phys. J. C* **82** (2022), no. 10 895, [[arXiv:2207.07636](#)].
- [16] **Belle-II** Collaboration, I. Adachi et al., *Evidence for $B^+ \rightarrow K + \nu\nu$ decays*, *Phys. Rev. D* **109** (2024), no. 11 112006, [[arXiv:2311.14647](#)].
- [17] D. Bečirević, G. Piazza, and O. Sumensari, *Revisiting $B \rightarrow K^{(*)} \nu \bar{\nu}$ decays in the Standard Model and beyond*, *Eur. Phys. J. C* **83** (2023), no. 3 252, [[arXiv:2301.06990](#)].
- [18] J. Rosiek, *Complete Set of Feynman Rules for the Minimal Supersymmetric Extension of the Standard Model*, *Phys. Rev. D* **41** (1990) 3464.
- [19] J. Rosiek, *Complete set of Feynman rules for the MSSM: Erratum*, [hep-ph/9511250](#).
- [20] V. De Romeri, K. M. Patel, and J. W. Valle, *Inverse seesaw mechanism with compact supersymmetry: Enhanced naturalness and light superpartners*, *Phys. Rev. D* **98** (2018), no. 7 075014, [[arXiv:1808.01453](#)].

- [21] H. An, P. S. B. Dev, Y. Cai, and R. N. Mohapatra, *Sneutrino Dark Matter in Gauged Inverse Seesaw Models for Neutrinos*, *Phys. Rev. Lett.* **108** (2012) 081806, [[arXiv:1110.1366](#)].
- [22] J. Kumar and M. Paraskevas, *Distinguishing between MSSM and NMSSM through $\Delta F = 2$ processes*, *JHEP* **10** (2016) 134, [[arXiv:1608.08794](#)].
- [23] Q.-Y. Hu, X.-Q. Li, Y.-D. Yang, and M.-D. Zheng, *$B_{s(d)} - \bar{B}_{s(d)}$ Mixing and $B_s \rightarrow \mu^+ \mu^-$ Decay in the NMSSM with the Flavour Expansion Theorem*, *JHEP* **06** (2019) 133, [[arXiv:1903.06927](#)].
- [24] T. Hahn, *Generating Feynman diagrams and amplitudes with FeynArts 3*, *Comput. Phys. Commun.* **140** (2001) 418–431, [[hep-ph/0012260](#)].
- [25] V. Shtabovenko, R. Mertig, and F. Orellana, *New Developments in FeynCalc 9.0*, *Comput. Phys. Commun.* **207** (2016) 432–444, [[arXiv:1601.01167](#)].
- [26] F. Staub, *SARAH 4 : A tool for (not only SUSY) model builders*, *Comput. Phys. Commun.* **185** (2014) 1773–1790, [[arXiv:1309.7223](#)].
- [27] T. Besmer and A. Steffen, *R-parity violation and the decay $b \rightarrow s$ gamma*, *Phys. Rev. D* **63** (2001) 055007, [[hep-ph/0004067](#)].
- [28] A. J. Buras, J. Girrbach-Noe, C. Niehoff, and D. M. Straub, *$B \rightarrow K^{(*)} \nu \bar{\nu}$ decays in the Standard Model and beyond*, *JHEP* **02** (2015) 184, [[arXiv:1409.4557](#)].
- [29] C. S. Kim, D. Sahoo, and K. N. Vishnudath, *Searching for signatures of new physics in $B \rightarrow K \nu \bar{\nu}$ to distinguish between Dirac and Majorana neutrinos*, *Eur. Phys. J. C* **84** (2024), no. 9 882, [[arXiv:2405.17341](#)].
- [30] X.-G. He, X.-D. Ma, and G. Valencia, *Revisiting models that enhance $B^+ \rightarrow K^+ \nu \bar{\nu}$ in light of the new Belle II measurement*, *Phys. Rev. D* **109** (2024), no. 7 075019, [[arXiv:2309.12741](#)].
- [31] **Belle Collaboration**, J. Grygier et al., *Search for $B \rightarrow h \nu \bar{\nu}$ decays with semileptonic tagging at Belle*, *Phys. Rev. D* **96** (2017), no. 9 091101, [[arXiv:1702.03224](#)].
[Addendum: *Phys.Rev.D* 97, 099902 (2018)].

- [32] B.-F. Hou, X.-Q. Li, M. Shen, Y.-D. Yang, and X.-B. Yuan, *Deciphering the Belle II data on $B \rightarrow K\nu\bar{\nu}$ decay in the (dark) SMEFT with minimal flavour violation*, *JHEP* **06** (2024) 172, [[arXiv:2402.19208](#)].
- [33] F.-Z. Chen, Q. Wen, and F. Xu, *Correlating $B \rightarrow K^{(*)}\nu\bar{\nu}$ and flavor anomalies in SMEFT*, *Eur. Phys. J. C* **84** (2024), no. 10 1012, [[arXiv:2401.11552](#)].
- [34] W. Altmannshofer, P. B. Dev, A. Soni, and Y. Sui, *Addressing $R_{D^{(*)}}$, $R_{K^{(*)}}$, muon $g - 2$ and ANITA anomalies in a minimal R -parity violating supersymmetric framework*, *Phys. Rev. D* **102** (2020), no. 1 015031, [[arXiv:2002.12910](#)].
- [35] J. A. Casas, A. Lleyda, and C. Munoz, *Strong constraints on the parameter space of the MSSM from charge and color breaking minima*, *Nucl. Phys. B* **471** (1996) 3–58, [[hep-ph/9507294](#)].
- [36] J. A. Casas and S. Dimopoulos, *Stability bounds on flavor violating trilinear soft terms in the MSSM*, *Phys. Lett. B* **387** (1996) 107–112, [[hep-ph/9606237](#)].
- [37] J. A. Casas, *Charge and color breaking*, [hep-ph/9707475](#). [*Adv. Ser. Direct. High Energy Phys.*21,469(2010)].
- [38] U. Ellwanger and C. Hugonie, *Constraints from charge and color breaking minima in the $(M+1)SSM$* , *Phys. Lett. B* **457** (1999) 299–306, [[hep-ph/9902401](#)].
- [39] M. S. Chanowitz, M. A. Furman, and I. Hinchliffe, *Weak Interactions of Ultraheavy Fermions. 2.*, *Nucl. Phys. B* **153** (1979) 402–430.
- [40] L. Durand, J. M. Johnson, and J. L. Lopez, *Perturbative Unitarity Revisited: A New Upper Bound on the Higgs Boson Mass*, *Phys. Rev. Lett.* **64** (1990) 1215.
- [41] J. Bernabeu, J. G. Korner, A. Pilaftsis, and K. Schilcher, *Universality breaking effects in leptonic Z decays*, *Phys. Rev. Lett.* **71** (1993) 2695–2698, [[hep-ph/9307295](#)].
- [42] S. Fajfer and A. Ilakovac, *Lepton flavor violation in light hadron decays*, *Phys. Rev. D* **57** (1998) 4219–4235.
- [43] A. Ilakovac, *Lepton flavor violation in the standard model extended by heavy singlet Dirac neutrinos*, *Phys. Rev. D* **62** (2000) 036010, [[hep-ph/9910213](#)].

- [44] A. Abada, J. Kriewald, E. Pinsard, S. Rosauero-Alcaraz, and A. M. Teixeira, *Heavy neutral lepton corrections to SM boson decays: lepton flavour universality violation in low-scale seesaw realisations*, *Eur. Phys. J. C* **84** (2024), no. 2 149, [arXiv:2307.02558].
- [45] **ATLAS** Collaboration, M. Aaboud et al., *Search for B - L R -parity-violating top squarks in $\sqrt{s} = 13$ TeV pp collisions with the ATLAS experiment*, *Phys. Rev. D* **97** (2018), no. 3 032003, [arXiv:1710.05544].
- [46] **CMS** Collaboration, A. M. Sirunyan et al., *Search for long-lived particles decaying into displaced jets in proton-proton collisions at $\sqrt{s} = 13$ TeV*, *Phys. Rev. D* **99** (2019), no. 3 032011, [arXiv:1811.07991].
- [47] **ATLAS** Collaboration, M. Aaboud et al., *Search for heavy charged long-lived particles in the ATLAS detector in 36.1 fb^{-1} of proton-proton collision data at $\sqrt{s} = 13$ TeV*, *Phys. Rev. D* **99** (2019), no. 9 092007, [arXiv:1902.01636].
- [48] **ATLAS** Collaboration, G. Aad et al., *Search for long-lived, massive particles in events with a displaced vertex and a muon with large impact parameter in pp collisions at $\sqrt{s} = 13$ TeV with the ATLAS detector*, *Phys. Rev. D* **102** (2020), no. 3 032006, [arXiv:2003.11956].
- [49] **ATLAS** Collaboration, G. Aad et al., *Search for R -parity-violating supersymmetry in a final state containing leptons and many jets with the ATLAS experiment using $\sqrt{s} = 13 \text{ TeV}$ proton-proton collision data*, *Eur. Phys. J. C* **81** (2021), no. 11 1023, [arXiv:2106.09609].
- [50] **CMS** Collaboration, A. M. Sirunyan et al., *Search for top squark production in fully-hadronic final states in proton-proton collisions at $\sqrt{s} = 13$ TeV*, *Phys. Rev. D* **104** (2021), no. 5 052001, [arXiv:2103.01290].
- [51] **CMS** Collaboration, A. Tumasyan et al., *Combined searches for the production of supersymmetric top quark partners in proton-proton collisions at $\sqrt{s} = 13$ TeV*, *Eur. Phys. J. C* **81** (2021), no. 11 970, [arXiv:2107.10892].
- [52] **ATLAS** Collaboration, M. Aaboud et al., *Search for supersymmetry in events with four or more leptons in $\sqrt{s} = 13$ TeV pp collisions with ATLAS*, *Phys. Rev. D* **98** (2018), no. 3 032009, [arXiv:1804.03602].

- [53] **ATLAS** Collaboration, M. Aaboud et al., *Search for lepton-flavor violation in different-flavor, high-mass final states in pp collisions at $\sqrt{s} = 13$ TeV with the ATLAS detector*, *Phys. Rev. D* **98** (2018), no. 9 092008, [[arXiv:1807.06573](#)].
- [54] **ATLAS** Collaboration, G. Aad et al., *Search for supersymmetry in events with four or more charged leptons in 139 fb^{-1} of $\sqrt{s} = 13$ TeV pp collisions with the ATLAS detector*, *JHEP* **07** (2021) 167, [[arXiv:2103.11684](#)].
- [55] **ATLAS** Collaboration, G. Aad et al., *Search for heavy Higgs bosons with flavour-violating couplings in multi-lepton plus b -jets final states in pp collisions at 13 TeV with the ATLAS detector*, *JHEP* **12** (2023) 081, [[arXiv:2307.14759](#)].
- [56] **Particle Data Group** Collaboration, S. Navas et al., *Review of particle physics*, *Phys. Rev. D* **110** (2024), no. 3 030001.
- [57] J. Aebischer, J. Kumar, P. Stangl, and D. M. Straub, *A Global Likelihood for Precision Constraints and Flavour Anomalies*, *Eur. Phys. J. C* **79** (2019), no. 6 509, [[arXiv:1810.07698](#)].
- [58] K. Earl and T. Grégoire, *Contributions to $b \rightarrow s\ell\ell$ Anomalies from R -Parity Violating Interactions*, *JHEP* **08** (2018) 201, [[arXiv:1806.01343](#)].
- [59] Q.-Y. Hu, Y.-D. Yang, and M.-D. Zheng, *Revisiting the B -physics anomalies in R -parity violating MSSM*, *Eur. Phys. J. C* **80** (2020), no. 5 365, [[arXiv:2002.09875](#)].
- [60] D. Bryman, V. Cirigliano, A. Crivellin, and G. Inguglia, *Testing Lepton Flavor Universality with Pion, Kaon, Tau, and Beta Decays*, [arXiv:2111.05338](#).
- [61] A. M. Coutinho, A. Crivellin, and C. A. Manzari, *Global Fit to Modified Neutrino Couplings and the Cabibbo-Angle Anomaly*, *Phys. Rev. Lett.* **125** (2020), no. 7 071802, [[arXiv:1912.08823](#)].
- [62] M. Blennow, P. Coloma, E. Fernández-Martínez, and M. González-López, *Right-handed neutrinos and the CDF II anomaly*, *Phys. Rev. D* **106** (2022), no. 7 073005, [[arXiv:2204.04559](#)].
- [63] **LHCb** Collaboration, R. Aaij et al., *Search for the rare decay $D^0 \rightarrow \mu^+\mu^-$* , *Phys. Lett. B* **725** (2013) 15–24, [[arXiv:1305.5059](#)].

- [64] **LHCb** Collaboration, R. Aaij et al., *Search for Rare Decays of D^0 Mesons into Two Muons*, *Phys. Rev. Lett.* **131** (2023), no. 4 041804, [[arXiv:2212.11203](#)].
- [65] **Belle** Collaboration, N. Tsuzuki et al., *Search for lepton-flavor-violating τ decays into a lepton and a vector meson using the full Belle data sample*, *JHEP* **06** (2023) 118, [[arXiv:2301.03768](#)].
- [66] S. Nandi, S. K. Patra, and A. Soni, *Correlating new physics signals in $B \rightarrow D^{(*)}\tau\nu_\tau$ with $B \rightarrow \tau\nu_\tau$* , [arXiv:1605.07191](#).
- [67] Q.-Y. Hu, X.-Q. Li, Y. Muramatsu, and Y.-D. Yang, *R-parity violating solutions to the $R_{D^{(*)}}$ anomaly and their GUT-scale unifications*, *Phys. Rev.* **D99** (2019), no. 1 015008, [[arXiv:1808.01419](#)].
- [68] G. Passarino and M. J. G. Veltman, *One Loop Corrections for e^+e^- Annihilation Into $\mu^+\mu^-$ in the Weinberg Model*, *Nucl. Phys.* **B160** (1979) 151–207.
- [69] A. Denner, *Techniques for calculation of electroweak radiative corrections at the one loop level and results for W physics at LEP-200*, *Fortsch. Phys.* **41** (1993) 307–420, [[arXiv:0709.1075](#)].
- [70] R. J. Dowdall, C. T. H. Davies, R. R. Horgan, G. P. Lepage, C. J. Monahan, J. Shigemitsu, and M. Wingate, *Neutral B -meson mixing from full lattice QCD at the physical point*, *Phys. Rev. D* **100** (2019), no. 9 094508, [[arXiv:1907.01025](#)].
- [71] J. T. Tsang and M. Della Morte, *B -physics from lattice gauge theory*, *Eur. Phys. J. ST* **233** (2024), no. 2 253–270, [[arXiv:2310.02705](#)].
- [72] **HFLAV** Collaboration, Y. S. Amhis et al., *Averages of b -hadron, c -hadron, and τ -lepton properties as of 2021*, *Phys. Rev. D* **107** (2023), no. 5 052008, [[arXiv:2206.07501](#)].
- [73] J. Albrecht, F. Bernlochner, A. Lenz, and A. Rusov, *Lifetimes of b -hadrons and mixing of neutral B -mesons: theoretical and experimental status*, *Eur. Phys. J. ST* **233** (2024), no. 2 359–390, [[arXiv:2402.04224](#)].
- [74] A. de Gouvea, S. Lola, and K. Tobe, *Lepton flavor violation in supersymmetric models with trilinear R -parity violation*, *Phys. Rev.* **D63** (2001) 035004, [[hep-ph/0008085](#)].

- [75] M. Misiak, A. Rehman, and M. Steinhauser, *Towards $\overline{B} \rightarrow X_s \gamma$ at the NNLO in QCD without interpolation in m_c* , *JHEP* **06** (2020) 175, [[arXiv:2002.01548](#)].
- [76] **HFLAV** Collaboration, Y. S. Amhis et al., *Averages of b -hadron, c -hadron, and τ -lepton properties as of 2018*, *Eur. Phys. J. C* **81** (2021), no. 3 226, [[arXiv:1909.12524](#)].
- [77] P. Arnan, D. Becirevic, F. Mescia, and O. Sumensari, *Probing low energy scalar leptoquarks by the leptonic W and Z couplings*, *JHEP* **02** (2019) 109, [[arXiv:1901.06315](#)].
- [78] **ALEPH, DELPHI, L3, OPAL, SLD, LEP Electroweak Working Group, SLD Electroweak Group, SLD Heavy Flavour Group** Collaboration, S. Schael et al., *Precision electroweak measurements on the Z resonance*, *Phys. Rept.* **427** (2006) 257–454, [[hep-ex/0509008](#)].
- [79] M.-D. Zheng, F.-Z. Chen, and H.-H. Zhang, *The $W\ell\nu$ -vertex corrections to W -boson mass in the R -parity violating MSSM*, *AAPPS Bull.* **33** (2023), no. 1 16, [[arXiv:2204.06541](#)].
- [80] E. Fernandez-Martinez, J. Hernandez-Garcia, and J. Lopez-Pavon, *Global constraints on heavy neutrino mixing*, *JHEP* **08** (2016) 033, [[arXiv:1605.08774](#)].
- [81] S. Heinemeyer, W. Hollik, and G. Weiglein, *Electroweak precision observables in the minimal supersymmetric standard model*, *Phys. Rept.* **425** (2006) 265–368, [[hep-ph/0412214](#)].
- [82] W. Porod, *SPheno, a program for calculating supersymmetric spectra, SUSY particle decays and SUSY particle production at e^+e^- colliders*, *Comput. Phys. Commun.* **153** (2003) 275–315, [[hep-ph/0301101](#)].
- [83] W. Porod and F. Staub, *SPheno 3.1: Extensions including flavour, CP-phases and models beyond the MSSM*, *Comput. Phys. Commun.* **183** (2012) 2458–2469, [[arXiv:1104.1573](#)].
- [84] I. Esteban, M. C. Gonzalez-Garcia, M. Maltoni, I. Martinez-Soler, J. a. P. Pinheiro, and T. Schwetz, *NuFit-6.0: updated global analysis of three-flavor neutrino oscillations*, *JHEP* **12** (2024) 216, [[arXiv:2410.05380](#)].

- [85] I. Esteban, M. Gonzalez-Garcia, M. Maltoni, T. Schwetz, and A. Zhou, *The fate of hints: updated global analysis of three-flavor neutrino oscillations*, *JHEP* **09** (2020) 178, [[arXiv:2007.14792](#)].
- [86] J. S. Alvarado and R. Martinez, *PMNS matrix in a non-universal $U(1)_X$ extension to the MSSM with one massless neutrino*, [arXiv:2007.14519](#).
- [87] **ATLAS** Collaboration, G. Aad et al., *Combined measurements of Higgs boson production and decay using up to 80 fb^{-1} of proton-proton collision data at $\sqrt{s} = 13\text{ TeV}$ collected with the ATLAS experiment*, *Phys. Rev. D* **101** (2020), no. 1 012002, [[arXiv:1909.02845](#)].
- [88] **ATLAS** Collaboration, G. Aad et al., *Search for heavy Higgs bosons decaying into two tau leptons with the ATLAS detector using pp collisions at $\sqrt{s} = 13\text{ TeV}$* , *Phys. Rev. Lett.* **125** (2020), no. 5 051801, [[arXiv:2002.12223](#)].
- [89] **ATLAS** Collaboration, G. Aad et al., *Search for charged Higgs bosons decaying into a top quark and a bottom quark at $\sqrt{s} = 13\text{ TeV}$ with the ATLAS detector*, *JHEP* **06** (2021) 145, [[arXiv:2102.10076](#)].
- [90] **LHCb** Collaboration, R. Aaij et al., *Amplitude analysis of $B_s^0 \rightarrow K_S^0 K^\pm \pi^\mp$ decays*, *JHEP* **06** (2019) 114, [[arXiv:1902.07955](#)].
- [91] R. Barbier et al., *R-parity violating supersymmetry*, *Phys. Rept.* **420** (2005) 1–202, [[hep-ph/0406039](#)].
- [92] R. Adhikari and G. Omanovic, *LSND, solar and atmospheric neutrino oscillation experiments, and R-parity violating supersymmetry*, *Phys. Rev. D* **59** (1999) 073003.
- [93] D. Chang, W.-F. Chang, M. Frank, and W.-Y. Keung, *The Neutron electric dipole moment and CP violating couplings in the supersymmetric standard model without R-parity*, *Phys. Rev. D* **62** (2000) 095002, [[hep-ph/0004170](#)].
- [94] N. Yamanaka, T. Sato, and T. Kubota, *Linear programming analysis of the R-parity violation within EDM-constraints*, *JHEP* **12** (2014) 110, [[arXiv:1406.3713](#)].

- [95] A. Abada, M. E. Krauss, W. Porod, F. Staub, A. Vicente, and C. Weiland, *Lepton flavor violation in low-scale seesaw models: SUSY and non-SUSY contributions*, *JHEP* **11** (2014) 048, [[arXiv:1408.0138](#)].
- [96] J. Chang, K. Cheung, H. Ishida, C.-T. Lu, M. Spinrath, and Y.-L. S. Tsai, *A supersymmetric electroweak scale seesaw model*, *JHEP* **10** (2017) 039, [[arXiv:1707.04374](#)].